01 Dec 2010

Geophysics at the Interface: Response of Geophysical Properties to Solid-Fluid, Fluid-Fluid, and Solid-Solid Interfaces

Rosemary Knight

Laura J. Pyrak-Nolte

Lee D. Slater

Estella A. Atekwana
Missouri University of Science and Technology, atekwana@mst.edu

et. al. For a complete list of authors, see https://scholarsmine.mst.edu/geosci_geo_peteng_facwork/1300

Recommended Citation

R. Knight and L. J. Pyrak-Nolte and L. D. Slater and E. A. Atekwana and A. L. Endres and J. T. Geller and D. P. Lesmes and S. Nakagawa and A. Revil and M. M. Sharma and C. Straley, "Geophysics at the Interface: Response of Geophysical Properties to Solid-Fluid, Fluid-Fluid, and Solid-Solid Interfaces," *Reviews of Geophysics*, vol. 48, no. 4, American Geophysical Union (AGU), Dec 2010.
The definitive version is available at https://doi.org/10.1029/2007RG000242

GEOPHYSICS AT THE INTERFACE: RESPONSE OF GEOPHYSICAL PROPERTIES TO SOLID-FLUID, FLUID-FLUID, AND SOLID-SOLID INTERFACES

R. Knight,[1] L. J. Pyrak-Nolte,[2] L. Slater,[3] E. Atekwana,[4] A. Endres,[5] J. Geller,[6] D. Lesmes,[7] S. Nakagawa,[6] A. Revil,[8,9] M. M. Sharma,[10] and C. Straley[11]

Received 20 August 2007; revised 30 January 2010; accepted 3 March 2010; published 2 December 2010.

[1] Laboratory studies reveal the sensitivity of measured geophysical properties to solid-fluid, fluid-fluid, and solid-solid interfaces in granular and fractured materials. In granular materials, electrical properties and nuclear magnetic resonance relaxation times exhibit a strong dependence on the size and properties of the solid-fluid interface. The electrical and seismic properties of granular materials and the seismic properties of fractured materials reveal a dependence on the size or geometry of fluid-fluid interfaces. Seismic properties of granular and fractured materials are affected by the effective stress and cementing material at solid-solid interfaces. There have been some recent studies demonstrating the use of field-scale measurements to obtain information about pore-scale interfaces. In addition, a new approach to geophysical field measurements focuses on the geophysical response of the field-scale interface itself, with successful applications in imaging the water table and a redox front. The observed sensitivity of geophysical data to interfaces highlights new ways in which geophysical measurements could be used to obtain information about subsurface properties and processes.

Citation: Knight, R., et al. (2010), Geophysics at the interface: Response of geophysical properties to solid-fluid, fluid-fluid, and solid-solid interfaces, *Rev. Geophys.*, *48*, RG4002, doi:10.1029/2007RG000242.

1. INTRODUCTION

[2] The Critical Zone is defined by *National Research Council* [2001, p. 35] as the "surface and near-surface environment [that] sustains nearly all terrestrial life" and is highlighted in the report as a research focus of particular urgency, given the rapidly expanding needs of society. There are numerous challenges that must be addressed in order to advance our understanding of this region of Earth. One key challenge is making the in situ measurements required to study the coupled physical, chemical, biological, and geological processes within the Critical Zone. The region is highly heterogeneous with properties and processes that vary in complex ways across a wide range of spatial and temporal scales. While methods exist for directly sampling this region, such methods can disrupt the system of interest and can rarely, if ever, provide the sampling (spatial or temporal) required to fully understand the complex, interrelated processes that operate in the Critical Zone.

[3] Over the past decade, we have seen increasing use of geophysical methods to noninvasively sample, or image, the "near-surface" (top ~100 m) part of the Critical Zone. An excellent review of these methods and their applications in the near surface is given by *National Research Council* [2000]. Geophysical methods can complement other, more traditional methods of subsurface characterization, such as the digging of trenches or the drilling of boreholes to acquire data or extract samples. They can provide scales of spatial and temporal resolution and coverage that cannot be

[1]Department of Geophysics, Stanford University, Stanford, California, USA.
[2]Department of Physics and Department of Earth and Atmospheric Sciences, Purdue University, West Lafayette, Indiana, USA.
[3]Department of Earth and Environmental Sciences, Rutgers, State University of New Jersey, Newark, New Jersey, USA.
[4]Boone Pickens School of Geology, Oklahoma State University, Stillwater, Oklahoma, USA.
[5]Department of Earth and Environmental Sciences, University of Waterloo, Waterloo, Ontario, Canada.
[6]Earth Sciences Division, Lawrence Berkeley National Laboratory, Berkeley, California, USA.
[7]Office of Biological and Environmental Research, U.S. Department of Energy, Washington, D. C., USA.
[8]Department of Geophysics, Colorado School of Mines, Golden, Colorado, USA.
[9]Also at Equipe Volcan, LGIT, CNRS UMR 5559, Université de Savoie, Le-Bourget-du-Lac, France.
[10]Department of Petroleum and Geosystems Engineering, University of Texas at Austin, Austin, Texas, USA.
[11]NMR Consultant, Ridgefield, Connecticut, USA.

8755-1209/10/2007RG000242
Paper number 2007RG000242

achieved with other methods. In addition, surface-based geophysical methods are noninvasive, so they do not disturb the region/process of interest. Recent applications of geophysical methods for Critical Zone studies have involved monitoring of (1) moisture dynamics and solute transport in the vadose zone, (2) biogeochemical transformations, (3) contaminant transport, (4) groundwater–surface water interaction, (5) carbon gas production and emissions in soils, and (6) mass movements and slope failure. As an example, Figure 1 shows ground-penetrating radar (GPR) images, acquired by *Hwang et al.* [2008], that are interpreted as capturing, by recording changes in the amount of reflected energy (displayed as instantaneous amplitude), the movement of an organic contaminant; such images are being used to study contaminant fate and transport. To effectively use geophysical measurements for any application, however, requires an understanding of the links between the imaged or measured geophysical properties and the material properties and processes in the near-surface region. For the example in Figure 1 we could ask, *Why* does the contaminant cause the observed variation in the geophysical images? Or the more general question that we could ask for all other Critical Zone studies is, What information about subsurface properties and processes is captured in the measured geophysical property?

[4] The link between measured geophysical properties and near-surface properties and processes is the focus of this paper. An excellent general introduction to this topic is given by *Guéguen and Palciauskas* [1994] and *Mavko et al.* [1998]. Material specific to the near-surface environment is given by *Knight and Endres* [2005] and *Santamarina et al.* [2005]. As is apparent in these references and in many earlier publications on this topic, the study of geophysical properties has typically focused on the ways in which the volume fractions and bulk properties of the components (solids and fluids) making up a material control its geophysical properties. As a result, the primary use of geophysical methods for Critical Zone studies has been on extracting, from the measured geophysical properties, information about the large-scale structure of the subsurface or estimates of the *volumes* of components (e.g., porosity, water content, and clay content). But laboratory-scale studies, designed to investigate the links between geophysical properties and subsurface properties/processes, provide evidence that geophysical measurements contain far more information about sampled geologic materials. In particular, as is the focus of this paper, a number of laboratory studies of granular and fractured materials have clearly demonstrated that geophysical measurements contain information about the *interfaces* between components in these materials, interfaces which we refer to as solid-fluid, fluid-fluid, and solid-solid. In fact, in many cases the processes occurring at interfaces and the properties of interfaces can dominate the geophysical response. The recognition that geophysical properties contain information about interfaces in granular and fractured materials raises the potential to use geophysical measurements in new and innovative ways to study Critical Zone properties and processes.

[5] In Figure 2 we show schematically the types of materials included in this review, granular and fractured. A granular geologic material (unconsolidated soil or sediment or consolidated rock) can be described as being composed of a solid phase (grains and cementing materials) and a fluid phase (gas or liquid). A fracture is a mechanical discontinuity that can occur in consolidated as well as unconsolidated material. Also shown in Figure 2 are the three types of interfaces covered in this review, solid-fluid, fluid-fluid, and solid-solid. Our main focus is the link between geophysical properties and the properties/processes at these interfaces at the pore scale; the one interface that we discuss at larger scales is the fluid-fluid interface. We treat the interfaces in granular materials and in fractures separately to illustrate their respective effects on geophysical properties. In a fractured granular material, we expect these effects to be superimposed; thus, the measured geophysical properties would contain contributions from interfaces both in the granular material and within the fractures. We begin by defining the three types of interfaces and discussing their roles in Critical Zone properties and processes.

[6] Let us first consider the solid-fluid interface: how could we use information about this interface in studying the Critical Zone? The solid-fluid interface, in granular and fractured materials, is defined as the region of contact between the solid phase and the fluids, contained in the pore spaces in a granular material and contained in the asperities (void spaces) in a fracture. In the top ~100 m of Earth, the solid-fluid interface has a direct impact on processes such as groundwater flow, geochemical reactions, contaminant transport, biogeochemical reactions, and many other Earth processes that are key to determining the properties. If we could extract, from geophysical measurements, information about the solid-fluid interface, this would be useful for many aspects of Critical Zone science.

Figure 1. Ground-penetrating radar images obtained by *Hwang et al.* [2008] (a) before and (b–f) after the release of an organic contaminant (50 L of a chlorinated solvent) 1.8 m below the ground surface at Canadian Forces Base Borden. The data are presented as the instantaneous amplitude, which is a measure of the amount of energy being reflected back from subsurface locations and recorded. The box outlines the region of solvent layer development. The prerelease image (Figure 1a) shows the low instantaneous amplitude values in the uncontaminated aquifer. The early time images (1/2 day (Figure 1b), 1 day (Figure 1c), and 2 weeks (Figure 1d)) found significant increases in instantaneous amplitude, attributed to solvent layer formation immediately after the release. As the dissolution of chlorinated solvents occurred, the instantaneous amplitude within the solvent layer was significantly reduced after 29 months (Figure 1e), with the image becoming very similar to the prerelease image by the end of the 66 months (Figure 1f). Reprinted from *Hwang et al.* [2008], copyright 2008, with permission from Elsevier.

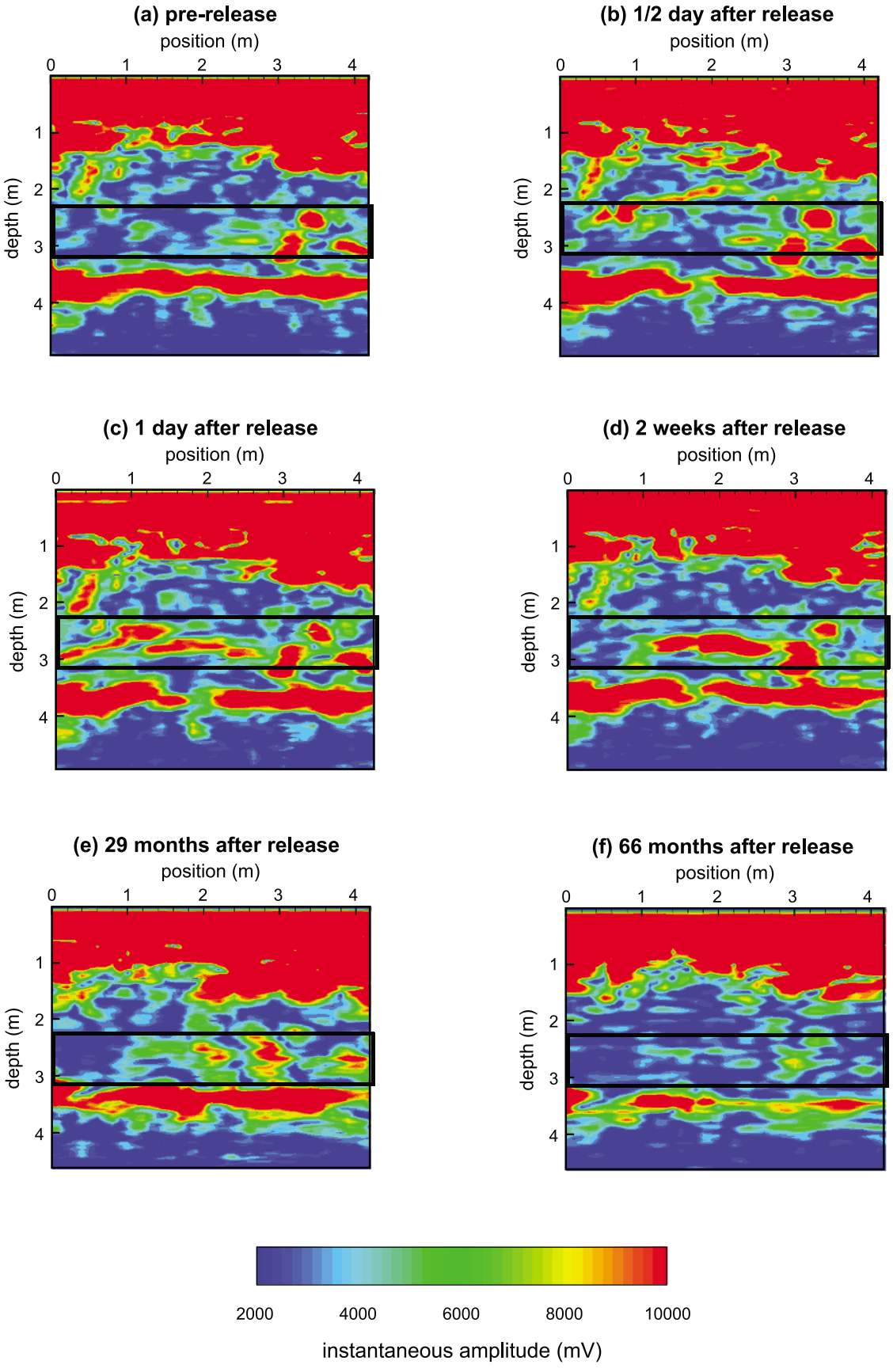
(a) pre-release
(b) 1/2 day after release
(c) 1 day after release
(d) 2 weeks after release
(e) 29 months after release
(f) 66 months after release
position (m)
depth (m)
0
1
2
3
4
2000
4000
6000
8000
10000
instantaneous amplitude (mV)

Figure 1

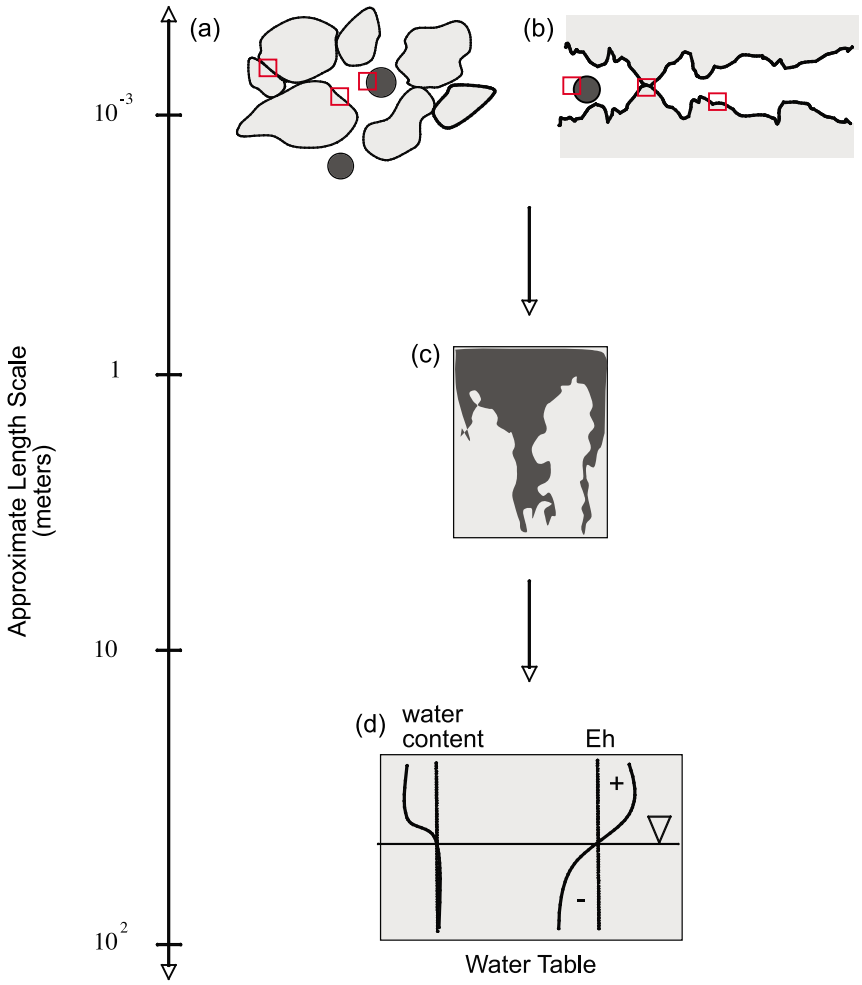

Figure 2. Schematic illustration of the materials, interfaces, and scales considered in this review. We represent the pore scale in (a) granular and (b) fractured material as a solid phase (shaded) containing a wetting fluid (white) and a second immiscible fluid (solid circles). The three types of interfaces are defined as solid-fluid, fluid-fluid, and solid-solid, with an example of each contained in the open squares. Fluid-fluid interfaces are considered at larger scales, shown here as (c) an immiscible displacement front at the scale of meters and (d) the water table at the scale of tens of meters.

[7] As an example, permeability (k) is the material property that governs the movement of fluids throughout the Critical Zone. Quantifying permeability is very challenging because of the heterogeneous nature of the subsurface and the way in which permeability varies with scale. The methods currently employed involve either laboratory measurements on samples taken from boreholes or aquifer testing (pump tests or tracer tests). The former provides estimates of permeability at a limited number of locations, at the scale of centimeters. The latter provides estimates of permeability averaged over tens of meters to hundreds of meters. An alternate approach would be to quantify the size of the solid-fluid interface, which is related to permeability as shown, for example, in the Kozeny-Carman equation [*Kozeny*, 1927; *Carman*, 1956]:

$$k = \frac{\phi^3}{5(1-\phi)^2 S_{sv}^2}, \quad (1)$$

where ϕ is porosity and S_{sv}, referred to as the specific surface, is defined as the surface area per solid volume. In a water-saturated material the size of the solid-fluid interface is equivalent to S_{sv}. If we could quantify the size of the solid-fluid interface with a geophysical measurement, this would provide a means of estimating permeability noninvasively and at the spatial resolution and coverage that can be obtained with geophysical field methods.

[8] Other applications where information about the solid-fluid interface would be of great value include studies of the geochemical reactions occurring in the Critical Zone. These reactions have wide-ranging impacts governing, for example, the quality of fresh water, the development of soils and distribution of plant nutrients, the integrity of underground waste repositories, and the geochemical cycling of elements [*Hochella and White*, 1990]. The size and composition of the solid-fluid interface directly affects reaction rates, and reactions, in turn, affect the size and composition of the interface, both of which are likely to change as a reaction progresses. The ability to use geophysical methods to quantify the size of the solid-fluid interface or to monitor changes

in the size or composition of the interface could dramatically change the approach to studying and monitoring geochemical processes in the Critical Zone.

[9] Many biogeochemical processes, concentrated in the Critical Zone as a result of the abundance of electron acceptors and nutrients, also profoundly impact, and are affected by, the size and state of the solid-fluid interface. Biogeochemical reactions play a fundamental role in the cycling of elements and the formation of minerals [e.g., *Hiebert and Bennett*, 1992]. Microbes themselves have the potential to modify the solid-fluid interface during early stages of microbial colonization of mineral surfaces (e.g., increasing surface roughness as well as surface area) and subsequently through the development of biofilms and biomats. Furthermore, microbial metabolism can enhance dissolution of certain mineral phases at the solid-fluid interface [e.g., *Hiebert and Bennett*, 1992; *McMahon et al.*, 1992, 1995; *Bennett et al.*, 1996] or drive the precipitation of secondary mineral phases onto the solid-fluid interface. Again, the use of geophysics to detect the microbially driven alteration of the solid-fluid interface could dramatically improve understanding of complex biogeochemical processes occurring in the Critical Zone at spatiotemporal scales unachievable with existing microbiological and biogeochemical methods. The potential for geophysical detection of biogeochemical processes occurring in Earth is discussed in detail in a recent review by *Atekwana and Slater* [2009].

[10] The pore spaces within a granular material and the apertures (void spaces) within a fracture can contain two or more fluid phases, thus giving rise to fluid-fluid interfaces. The fluid-fluid interface is the region of contact between two immiscible fluid phases. As shown in Figure 2, the fluid-fluid interface is the one interface that we have elected to consider at multiple scales. We start at the pore scale then move up to the scale of meters, where our example is an immiscible displacement front, then up to the scale of tens of meters, where our example is the water table, treated as equivalent to the top of the saturated zone so defined by a change in water content and a change in redox potential.

[11] As discussed for the solid-fluid interface, the fluid-fluid interface also plays an important role in determining Earth processes and is modified by these processes. One Critical Zone fluid-fluid interface is that associated with the interface between water and air in the vadose zone. This is an important interface in soil physics and hydrology as its geometry is diagnostic of the moisture content and water available to support plant growth. It is well recognized that the geometry of this interface is a function not just of soil saturation but also of saturation history. The complex redistribution of moisture during wetting versus drying complicates studies of vadose zone hydrology and soil moisture dynamics as capillary suction (and thus moisture transport) is not simply predicted from volumetric moisture content alone. Hysteresis in curves of matric potential versus moisture content observed between wetting and drying cycles is evidence for a redistribution of the air-water interface that is commonly observed in soil studies. Interestingly, as discussed in this review, such hysteresis has also been documented in electrical and seismic geophysical measurements, with implications for improving studies of soil moisture dynamics over studies based on volumetric measurements (diagnostic of moisture content only) alone.

[12] Other types of fluid-fluid interfaces exist in the near surface because of anthropogenic activities that result in the mixing of fluids. The spread of a contaminant in the subsurface and the processes involved in removing or immobilizing the contaminant all produce complex patterns of fluid saturation and associated fluid-fluid interfaces. Much effort has been expended over the past 20 years developing effective methods of site characterization to design and monitor contaminant cleanup and remediation. These methods have focused on mapping out spatial and temporal variations in the volume fraction of the contaminant. A new approach would be to map the location of the fluid-fluid interface between a contaminant and the background water/air and monitor its changing geometry over time, using the unique signature of the fluid-fluid interface itself. Recent laboratory studies hold promise for developing new ways of using geophysical methods for this purpose.

[13] The third interface that we consider is the solid-solid interface. In a granular material, the solid-solid interface refers to the region of contact between grains. The grain-to-grain contacts can be partially or completely in contact and can be welded and/or cemented. A fracture in a consolidated material can be thought of as two half-spaces in partial contact where the contacts are solid-solid interfaces. When fractures exist in a granular material, grain-to-grain contacts bridge across the fracture and also occur within the material on either side of the fracture.

[14] Solid-solid interfaces have a direct control on the mechanical properties of granular and fractured materials because these interfaces control the mechanical coupling between grains and across fractures. Studies of near-surface processes that are controlled by, and control, the mechanical properties require information about the way in which the coupling across the solid-solid interface changes with time and is affected by other processes and in situ conditions. For weakly coupled grain contacts or fractures, a small physical modification of the solid-solid interface due to stress, pore pressure, fluid content, or geochemical or biogeochemical processes can lead to failure of granular material resulting in, for example, slope failure, physical weathering and soil development, faulting and fracturing, and liquefaction [e.g., *Wang and Sassa*, 2003]. The solid-solid interface is also closely tied to the hydraulic properties of a material; the extent of solid-solid contact affects both the connectivity and tortuosity of the void space. As a consequence, changes in the solid-solid interface can result in significant changes in flow paths. The loss of contact across this interface, for example, can result in the formation of new flow paths. The ability to remotely acquire information about the coupling at solid-solid interfaces could therefore assist in studying many processes that occur in the Critical Zone. As discussed in this review, several researchers have shown that the state of the contact (e.g., dry, fluid filled, cemented, or partially cemented) affects the elastic moduli of a material and, in

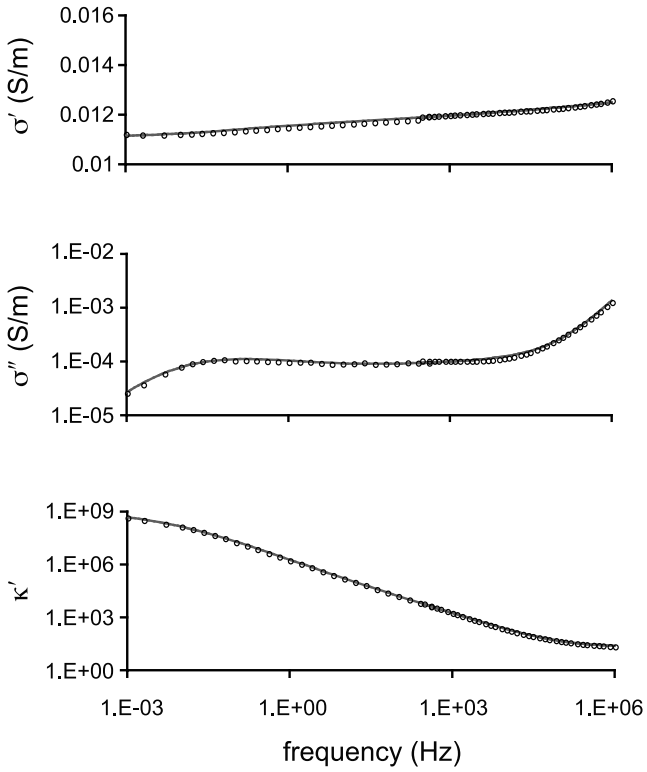

Figure 3. The observed frequency dependence of the electrical properties, σ', σ'', and κ', of Berea sandstone saturated with 0.01 M NaCl [from *Lesmes and Frye*, 2001].

turn, its geophysical response, thus raising the possibility that geophysical measurements could provide such information for Critical Zone studies.

[15] Geophysical methods have been used, increasingly, over the past decade for Critical Zone studies. But the focus has been on extracting, from the geophysical data, information about the large-scale structure of the subsurface or estimates of the *volumes of components*. Of great interest to us, and the motivation for this review, is the link between geophysical data and the *interfaces between components*. In sections 3–5 we present examples of laboratory studies of granular and fractured materials illustrating the effects of interfaces on the geophysical properties which have been found to be sensitive to solid-fluid, fluid-fluid, and solid-solid interfaces: electrical properties, nuclear magnetic resonance (NMR) relaxation time constants, and seismic properties. We do not consider magnetic and gravity potential field measurements as there are no laboratory studies that reveal a link between these geophysical measurements and the properties of interfaces. Throughout, we ask the question, What information can we obtain about interfaces from geophysical measurements? While much of this paper is a review of existing data (some acquired 10–20 years ago), the process of bringing together and considering electrical, NMR, and seismic data has allowed us to highlight the ways in which geophysical measurements could be used in new ways to obtain information about interfaces, across a range of scales, in both granular and fractured materials. We conclude by reviewing the current progress being made in taking these laboratory-scale findings to the field scale, where the ability to characterize interfaces with noninvasive, high-resolution geophysical imaging methods would lead to significant advances in studies of the subsurface and could provide the information needed about the region of Earth referred to as the Critical Zone.

2. DEFINITION OF GEOPHYSICAL PROPERTIES

[16] The geophysical properties reviewed in this paper are those that have shown a sensitivity to solid-fluid, solid-solid, and/or fluid-fluid interfaces: electrical properties, NMR relaxation time constants, and seismic properties. We here define these properties and introduce the terminology used in this review.

[17] The electrical properties of geological materials are typically measured in the laboratory across the frequency range from DC to ~1 GHz, which coincides with that used in field systems. The nomenclature used in the literature to refer to the electrical properties of geologic materials is highly variable and can be a source of confusion in trying to compare and understand the results from different studies. Adopting the nomenclature described in detail by *Knight and Endres* [2005], we represent the response of a material to an applied electric field using the complex electrical conductivity σ:

$$\sigma(\omega) = \sigma'(\omega) + i\sigma''(\omega), \tag{2}$$

where the real part σ' represents energy lost and the imaginary part σ'' represents energy stored; ω is frequency. Two terms used to describe the electrical properties are the electrical conductivity, which refers to σ', and the dielectric constant κ', which is related to σ'' through the following equality:

$$\kappa' = \frac{\sigma''}{\varepsilon_0 \omega}, \tag{3}$$

where ε_0 is the permittivity of free space. To illustrate the way in which electrical properties vary with frequency, we show in Figure 3 [from *Lesmes and Frye*, 2001] the results from laboratory measurements on Berea sandstone (a quarried rock), saturated with 0.01 *M* NaCl. Plotted as a function of frequency from 10^{-3} to 10^{6} Hz are the three measured parameters commonly reported in laboratory studies: σ', σ'', and κ'. The parameter referred to as DC conductivity, σ_{DC}, is the value of σ' as $\omega \rightarrow 0$. The parameter referred to as κ'_{GHz} is the value of κ' as ω approaches the relaxation frequency (~10 GHz) of bulk water. As discussed in greater detail in sections 3.1 and 4.1, measurements of electrical properties have been found to be very sensitive to the properties of solid-fluid and fluid-fluid interfaces in granular materials.

[18] In addition to the geophysical estimation of the electrical properties summarized above, it is also possible to make geophysical measurements of electrical current flows

associated with coupled processes that occur in geologic materials. These measurements, known as self-potentials (i.e., the potentials of an internal electric field), are attributed to a number of mechanisms generating sources of electric current in the subsurface. Interestingly, most of these sources can be closely associated with interfaces. Perhaps the most extensively studied mechanism in relation to Critical Zone processes is the streaming current source term resulting from the transport of excess charge in the electrical double layer at the solid-fluid interface of a geologic material in response to the viscous drag exerted by fluid flow through the pores. The resulting streaming potential recorded at the Earth surface is unique in that this geophysical signature is exclusively generated at the solid-fluid interface. Another self-potential source mechanism is electrodiffusion, arising because of gradients in the chemical potentials of charge carriers. Electrodiffusion is affected by the electrical double layer because the presence of the electrical double layer changes the Hittorf numbers (the Hittorf number of an ion is the fraction of current carried by this ion) in the pore space, so it modifies the current density associated with the gradient of the chemical potential of the charge carriers [*Revil and Linde*, 2006]. Finally, geobatteries can develop when an electron conductor bridges electron donors and electron acceptors, resulting in current flow in response to the redox gradient [*Sato and Mooney*, 1960]. Geobatteries can generate remarkably large self-potentials and can be related to field-scale interfaces, as we show in section 6.3.

[19] Another geophysical property that shows pronounced sensitivity to the solid-fluid interface is measured using hydrogen NMR. Laboratory NMR relaxometry has been used in the Earth sciences for the past 30 years in the laboratory, to study the properties of water-saturated porous materials. The NMR measurement detects the hydrogen nuclei in the water. When a sample sits in a static magnetic field (B_0), a small net nuclear magnetization (M) develops in the direction of B_0, referred to as the z axis. M cannot be detected electronically while at equilibrium (along the z direction); it is necessary to disturb the equilibrium to observe M. In the NMR experiment a properly oriented radio frequency field, applied for a short duration at the Larmor frequency of hydrogen, serves to rotate M away from the z axis so that there is a component of M in the xy plane. This component of M in the xy plane is detectable. Specific time constants can be associated with the exponential return, or "relaxation," to equilibrium. Of interest in our review is the link between these relaxation time constants and the size and state of the solid-fluid interface in granular materials.

[20] Another very common form of geophysical measurement is the determination of the seismic properties of geological materials. The properties measured in both laboratory and field studies include the compressional wave (P wave) velocity V_p, shear wave (S wave) velocity V_s, the amplitudes of the elastic waves, and the attenuation. The material properties governing the wave velocities are the elastic moduli and the density, as shown in the following expressions:

$$V_p = \sqrt{\frac{B + \frac{4}{3}\mu}{\delta}} \tag{4}$$

$$V_s = \sqrt{\frac{\mu}{\delta}}, \tag{5}$$

where B is the bulk modulus, μ is the shear modulus, and δ is the density of a material.

[21] Wave attenuation in materials is often quantified using the seismic quality factor, Q, that is related to the energy dissipated per wave cycle relative to the total elastic energy of a wave cycle. Attenuation can be quantified by using either the seismic quality factor (equation (6)) or the seismic attenuation coefficient, α_s (equation (7)):

$$Q = \frac{\omega l}{2V_{\text{phase}} \ln(u/u_o)} \tag{6}$$

$$\alpha_s \approx \frac{\omega}{2V_{\text{phase}}Q}, \tag{7}$$

where V_{phase} is the material phase velocity, l is the sample length, and u/u_o is the transmission coefficient [*Pyrak-Nolte et al.*, 1990]. Experimentally, the quantity u/u_o is the ratio of spectral amplitudes for a sample relative to those for a standard. For additional details on calculating Q in granular material, see *Johnston et al.* [1979], *Bourbie et al.* [1987], or *Nihei* [1992].

[22] These defined geophysical properties have been measured, in the laboratory and the field, for many years and have been widely used in petroleum and mineral exploration, and increasingly for Critical Zone studies, to obtain information about *volumetric* parameters, such as the level of water saturation or porosity. The focus of this review is the sensitivity of these geophysical properties to *interfaces* in materials. Our review of the literature reveals many ways in which the electrical, NMR, and seismic properties of Earth materials can be used to probe behavior at solid-fluid, fluid-fluid, and solid-solid interfaces. These laboratory studies provide the basis for new ways of thinking about the use and interpretation of geophysical data from the Critical Zone.

3. SOLID-FLUID INTERFACE

[23] As discussed in section 1, the solid-fluid interface has a direct impact on many Critical Zone physical, chemical, and biological processes. There is great interest, therefore, in obtaining information about the solid-fluid interface. With this in mind, we review the laboratory studies that have revealed numerous links between the electrical properties and NMR response of geologic materials and the size and

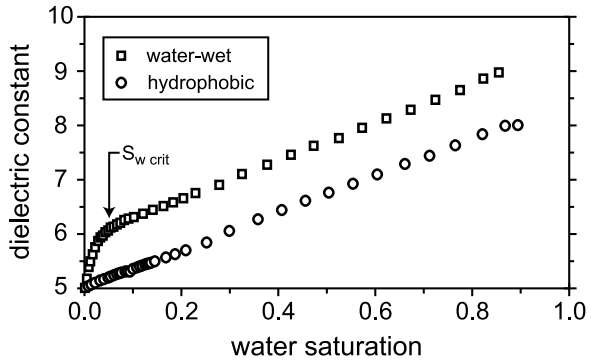

Figure 4. Data from *Knight and Abad* [1995] showing the change in dielectric constant κ' as the level of water saturation S_w decreased in a water-wet sandstone and a sample of the same sandstone chemically treated to make the mineral surfaces hydrophobic. $S_{w\ crit}$ corresponds to the presence of three to four monolayers of water coating the internal surface area of the sample.

state of the solid-fluid interface. These studies raise the possibility that geophysical field measurements of these geophysical properties could allow us to obtain key information about the solid-fluid interface and related properties.

3.1. Response of Electrical Measurements to the Solid-Fluid Interface in Granular Materials

[24] It is not surprising that electrical properties are sensitive to the solid-fluid interface, given the distinct electrical properties of the interface itself. The surfaces of all minerals in contact with a fluid have a net surface charge. In response to the net surface charge, ions (referred to as counterions) in the surrounding pore water migrate to the surface. The electrical double layer that forms at the solid-water interface includes the bound (Stern) layer of sorbed counterions and the diffuse (Gouy-Chapman) layer in which the counterions are influenced by the surface charge only through electrostatic interactions.

[25] Many of the past studies and uses of measurements of the electrical properties of geological materials focused on the links between the geophysical properties and the level of water saturation or porosity. The magnitudes of κ'_{GHz} and σ_{DC} for many water-saturated materials can be predicted reasonably well with models that only account for the volume fractions and bulk electrical properties of the two phases: the solid and the water. One such model used for κ'_{GHz} is the time propagation (TP) model [*Wharton et al.*, 1980]:

$$\sqrt{\kappa'_{\mathrm{GHz}}} = (1-\phi)\sqrt{\kappa'_s} + \phi\sqrt{\kappa'_w}, \tag{8}$$

where ϕ is porosity and κ'_s and κ'_w are the dielectric constants of the dry solid and the pore water, respectively. (The values of κ'_s and κ'_w are constant over the frequency range of DC to GHz.) At the other end of the frequency range, σ_{DC} of water-saturated materials is commonly modeled using Archie's law [*Archie*, 1942], which assumes that all of the conduction is through the movement of ions in the pore water:

$$\sigma_{\mathrm{DC}} = \phi^m \sigma_{\mathrm{DC\,water}}, \tag{9}$$

where $\sigma_{\mathrm{DC\ water}}$ is the DC conductivity of the pore water and m is referred to as the cementation exponent, which represents the level of connectivity of the pore space; the solid phase is assumed to act as an insulator. Archie found m to be close to 2 in his experiments on Gulf Coast sandstones and suggested that m would have a value of 1.3 in unconsolidated sands [*Archie*, 1942].

[26] The above expressions are valid for water-saturated materials when the dominant controls on the electrical properties are the volume fractions and bulk electrical properties of the solid and water phases. Both expressions, however, become increasingly inaccurate as the size of the solid-water interface increases and the properties of the interfacial region start to impact the electrical properties of the material. In the case of σ_{DC}, the ions in the electrical double layer at the solid-water interface provide an additional path for conduction. As the surface area increases, such as with the addition of clays, this can become the dominant part of the measured conductivity [*Waxman and Smits*, 1968]. The magnitude of σ_{DC} then shows a strong dependence on the surface area (or clay content) of a material, resulting in a relationship between σ_{DC} and clay content commonly observed in both laboratory and field data. In the case of dielectric properties, the presence of a solid surface has been found to reduce κ' of water from a value of 80 for bulk water to a value of ~6 in the first few monolayers (~1 nm) adjacent to the surface [*Bockris et al.*, 1966]. This causes κ'_{GHz} of water-saturated soils to decrease as the surface-area-to-volume ratio of the pore space (S/V_{pore}) increases [*Wang and Schmugge*, 1980].

[27] In the frequency range between DC and GHz, the presence of the solid-water interface has a large effect on the electrical property that represents the storage of energy, through the accumulation and/or orientation of charge, in response to an applied electric field. At higher frequencies, this property is typically reported as κ', while at lower frequencies, this storage term is typically reported as σ''. The impact of the solid-water interface on κ' in the frequency range of 50 kHz to 10 MHz is illustrated in Figure 4 (data taken from *Knight and Abad* [1995]), where we show the change observed in κ' as the level of water saturation S_w decreased (through drying) in both a water-wet sandstone (where water spontaneously coats the solid surface) and a sample of the same sandstone chemically treated to make the mineral surfaces hydrophobic. For the hydrophobic sample, across the entire saturation range, the decrease in S_w caused a decrease in κ' that is proportional to the decrease in water-filled porosity (i.e., κ' is accurately modeled with the TP model (equation (8))). In contrast, in the water-wet sandstone, there is a significant change in κ' across a region at low saturations defined as $0 < S_w < S_{w\ crit}$, with $S_{w\ crit}$ found to correspond to the presence of three to four monolayers of water coating the internal surface area of the

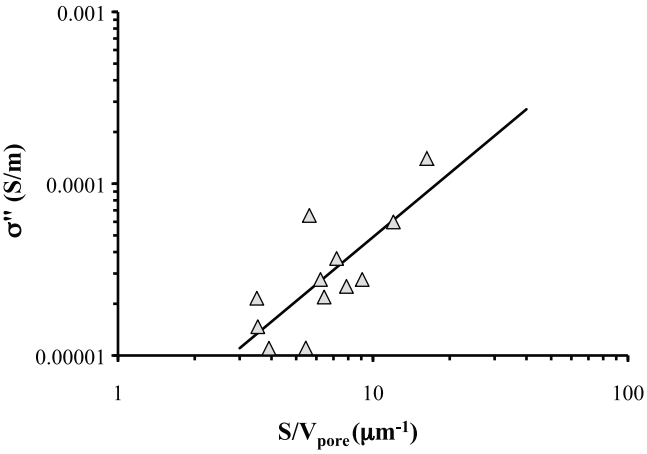

Figure 5. The relationship between σ'' of water-saturated sands and S/V_{pore} (modified after *Slater and Glaser* [2003]).

sample [*Knight and Endres*, 1990]. These data clearly illustrate the effect of the solid-water interface on dielectric properties: the addition of water wetting the solid surface causes a much greater increase in κ' than is caused by the addition of the same amount of water to the central volume of the pore space at higher saturations. The magnitude of κ' at $S_{w\ \text{crit}}$ increases with increasing S/V_{pore} in water-wet sandstones, resulting in a linear relationship between κ' and S/V_{pore} [*Knight and Nur*, 1987a].

[28] Similar observations of the link between the electrical properties of geological materials and the presence of the solid-water interface have been made at low frequencies. Laboratory measurements on water-saturated sandstones and sediments at ~1 Hz show a dependence of σ'' (the electrical property typically chosen to represent the storage of energy at these frequencies) on S/V_{pore} [*Börner and Schön*, 1991]. The form of this relationship can be seen in Figure 5 (modified after *Slater and Glaser* [2003]), where σ'' of water-saturated sands is plotted as a function of S/V_{pore}.

[29] The fact that in the frequency range of ~1 Hz to 10 MHz measured electrical properties are related to S/V_{pore} has led to laboratory studies that illustrate the potential use of electrical properties to estimate hydraulic conductivity K and permeability k [*Knoll et al.*, 1995; *Börner et al.*, 1996; *Slater and Lesmes*, 2002]. These hydraulic properties also depend on S/V_{pore} as expressed, for example, by the Kozeny-Carman equation [*Kozeny*, 1927; *Carman*, 1956].

[30] When the magnitudes of κ' and σ'' are largely determined by the water-wetted S/V_{pore}, any process that results in a change in the size of the water-wetted surface area should cause a change in κ' and σ''. This presents the intriguing possibility that monitoring a subsurface region with measurements of κ' and σ'' could allow us to study or monitor such processes. An example is the adsorption (or desorption) of an organic contaminant within the pore space of a water-wet material; this process decreases (or increases) the water-wetted surface area by exchanging organic molecules and water at the solid surface. This response was seen in the laboratory study of *C. Li et al.* [2001], where the adsorption of increasing amounts of hydrocarbon to the surfaces of kaolinite resulted in a corresponding decrease in κ' at a frequency of ~1 MHz. Measurements of σ' are also very sensitive to the wettability of a material, decreasing much more rapidly with decreasing water saturation for solid surfaces that are hydrophobic [*Sharma et al.*, 1991]. This is primarily because the conductive water phase loses continuity as its saturation decreases.

[31] Insights into the mechanisms responsible for the link between κ' and σ'' and S/V_{pore} can be gained by considering the way in which σ', σ'', and κ' vary with frequency. Descriptions of the frequency dependence of the electrical properties of geological materials have commonly used derivations of the Cole-Cole model [*Cole and Cole*, 1941], which describes the response of a system in terms of one or more mechanisms with defined relaxation time constants. For solid-water mixtures, theories have been proposed that relate the magnitude of κ' and σ'' to charge movement in both the bound and diffuse regions of the electrical double layer and recognize the role that the excess conductivity in the double layer can play [e.g., *Schwarz*, 1962; *Dukhin and Shilov*, 1974; *de Lima and Sharma*, 1992; *Endres and Knight*, 1993].

[32] One theoretical treatment of the response of water-saturated rocks and sediments considers the range of grain and pore sizes in a material and the movement and accumulation of charge at interfaces [*Lesmes and Morgan*, 2001]. When ions migrate through water-bearing rocks and soils they can accumulate at pore throat constrictions, at blockages caused by clay minerals, or on rough grain surfaces. The reequilibration of these accumulated charges is a diffusion-controlled process with an associated relaxation time constant. For example, in the case of polarization of spherical grains surrounded by an electrical double layer of charge, the diffusive relaxation time constant is defined by $\tau = R^2/2D$, where R is the grain radius and D is the surface diffusion coefficient [*Schwarz*, 1962]. The variation in κ' seen in Figure 3 can be thought of as a cumulative measure of diffusive polarization mechanisms, where larger-sized grains/pores are polarized as frequency decreases. The link to S/V_{pore} is through the relationships between grain/pore size and S/V_{pore}.

[33] Another approach is to model the frequency dependence of κ' as a power law dependence on frequency, recognized by *Jonscher* [1975] as a way of describing the electrical response of a wide range of materials. The change in κ' of a geological material across the frequency range ~50 kHz to ~1300 MHz has been found to be well described by the following expression [*Knight and Nur*, 1987a; *Taherian et al.*, 1990]:

$$\kappa' = a\,\omega^{-\alpha}, \tag{10}$$

where a and α are empirically determined constants. The constant α at frequencies from 50 kHz to 4 MHz increases with S/V_{pore} [*Knight and Nur*, 1987a].

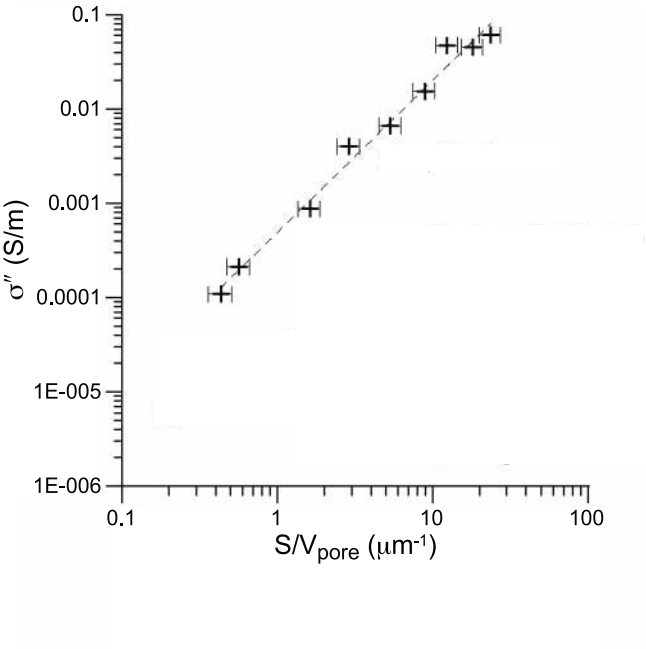

Figure 6. The dependence of σ'' on S/V_{pore} for water-saturated mixtures of sand and granular zero-valent iron (Fe_0) (modified after *Slater et al.* [2006]).

[34] The double layer at the solid-water interface that controls the electrical frequency response of geologic materials plays a central role in the measured streaming potential, which is thereby implicitly related to the size of the solid-fluid interface. A streaming current density is generated because of the drag of excess electrical charge in the diffuse layer, while an electroosmotic contribution to fluid transport also results from the viscous drag of pore water associated with displacement of electrical charge in an electric field. The coupling between the electrical (φ) and pore fluid potentials (p) is described by a coupling coefficient, $C = \partial\phi/\partial p$, taken at a total current density equal to 0, that is traditionally related to the zeta potential of the electrical double layer forming at the solid-fluid interface via the Helmholtz-Smoluchowski equation (in the absence of surface conductivity). However, more recent work, primarily on clay minerals, has reformulated C (here expressed relative to hydraulic head instead of pore fluid pressure) in terms of the microgeometry of a porous medium,

$$C = -\frac{\bar{Q}_v K}{\sigma_{\text{DC}}}, \tag{11}$$

where $\bar{Q}_v$ is the excess charge of the diffuse layer per pore unit volume [*Bolève et al.*, 2007]. This new formulation shows that streaming potentials can be modeled in terms of the hydraulic properties of a porous medium [e.g., *Jardani and Revil*, 2009].

[35] The electrodiffusion effect can, in the presence of clay minerals, also offer insights into the size of the solid-fluid interface. Electrodiffusion potentials (arising because of gradients in the chemical potentials of charge carriers within pore fluids) are normally small in clay-free soils but can be enhanced by the unique ion exclusion capabilities of clay minerals. The strong dependence of this electrodiffusion effect on clay minerals provides a semiquantitative link between self-potentials and interfacial properties such as S/V_{pore} as clay minerals are characterized by very high surface areas.

[36] When metallic particles are present in geologic materials, there is an electrical response of the metal-water interface that is distinctly different from that of the solid-water interface for nonmetallic solids. Polarization at the metal-water interface consists of a diffusive component due to the movement of ions in the electrical double layer predominantly normal to the interface and an electrochemical component associated with the redox reactions required to promote energy transfer from ionic conduction in the pore fluid to electronic conduction in the metal and vice versa. Even though this polarization is unique to metallic particles, we again find that the magnitude of charge polarization at the metal-water interface is related to the surface area of the solid, in this case metal, phase. This can be seen in Figure 6, where we show the dependence of σ'' on S/V_{pore} for water-saturated mixtures of sand and granular zero-valent iron (Fe_0) [*Slater et al.*, 2006]. The electrolyte activity and the valence of the redox active ions in the electrical double layer are also important variables in controlling the response of the metal-water interface [*Slater et al.*, 2005].

[37] All of the above examples are taken from studies focused on understanding the relationships between geophysical properties and the physical and chemical properties of geologic materials. Only recently have researchers come to recognize the need to also consider the biological properties of materials when interpreting geophysical data. There is a relatively new field of "biogeophysics" within the near-surface geophysics community that explores how biogeochemical processes either directly or indirectly affect measured geophysical properties. For example, bacteria can play a critical role in determining the properties of the solid-water interface. Bacteria have a large surface area (~30–100 m^2/g) [*van der Wal et al.*, 1997a] and a reported counterion charge density for the bacterial cell wall of ~0.5–1.0 C/m^2 [*van der Wal et al.*, 1997b]. In favorable conditions, bacteria can form continuous biofilms, with electrical double layers with properties that are highly sensitive to fluid chemistry [*Daughney and Fein*, 1998; *Borrok et al.*, 2004; *Claessens et al.*, 2004; *Cox et al.*, 1999; *Martinez et al.*, 2002]. The presence of the bacteria and the associated microbe-mineral-fluid interactions can cause significant changes in the properties of the solid-water interface by controlling or accelerating processes that lead to changes in pore fluid chemistry, changes in surface area and pore geometry, and precipitation of new minerals. One example is silicate mineral weathering, where bacteria accelerate the process either directly by colonizing mineral surfaces or indirectly by the production of organic and inorganic acids that enhance the dissolution of minerals [e.g., *Hiebert and Bennett*, 1992].

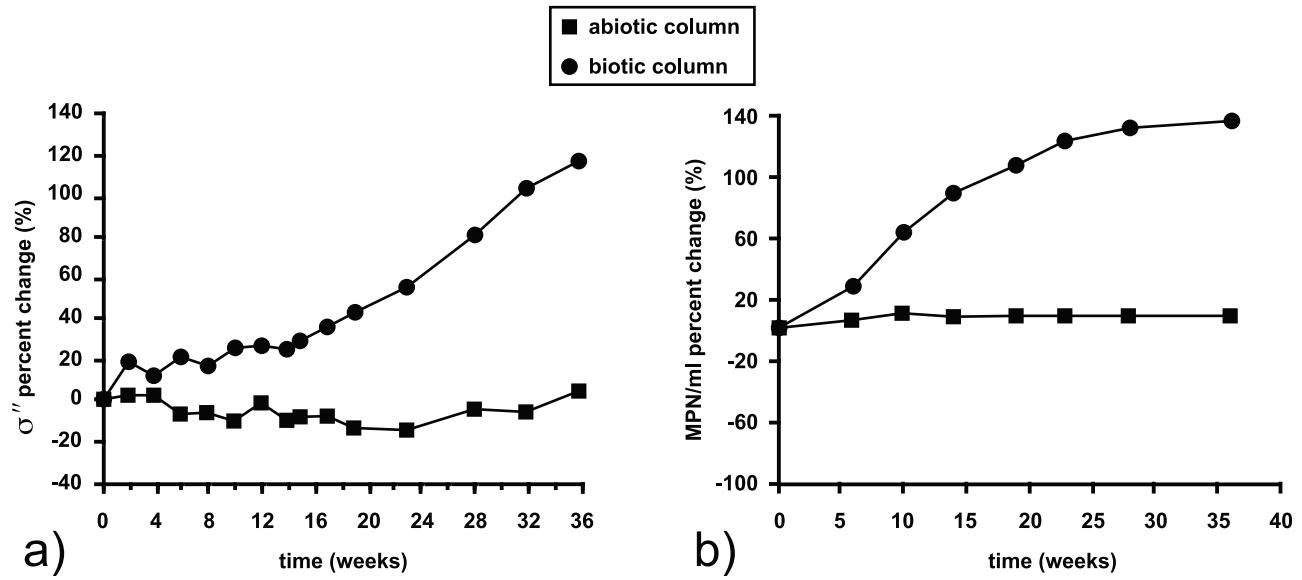

Figure 7. The observed percent changes in (a) σ'' and (b) microbial population numbers (MPN/ml) in biotic and abiotic columns [*Abdel Aal et al.*, 2004]. Note the correspondence between the increase in σ'' and the increase in MPN in the biotic columns.

[38] We show in Figure 7 data [from *Abdel Aal et al.*, 2004] that demonstrate the role of biological/biogeochemical processes in affecting solid-water interfaces and the measured electrical properties. During a laboratory investigation of the biodegradation of diesel fuel, an increase in σ'' was found to be concurrent with an increase in microbial population numbers in the biotic columns; no changes were observed in the abiotic columns. *Abdel Aal et al.* [2004] proposed that this increase in σ'' resulted from an increase in the surface area of the interface and an increase in surface charge density due to microbial attachment to the solid surface. In another study *Davis et al.* [2006] were able to document that changes in σ'' paralleled changes in microbial cell counts during a microbial growth experiment, suggesting that σ'' can be used to investigate microbial growth and biofilm formation in porous media. The results of these studies suggest yet another potential use of geophysical measurements at the field scale, in this case to study microbial processes such as biofilm formation or biomineralization that impact the solid-water interface. Biogeophysics represents one of the forefronts of near-surface geophysics, exploring the new links being found between geophysics and microbiology.

[39] In summary, laboratory studies of the electrical properties of geological materials have repeatedly shown a sensitivity of the measured geophysical properties to the presence and state of the solid-water interface. While we still lack a complete understanding of the way in which the solid-water interface governs the magnitude and frequency dependence of electrical properties, there is no doubt that these geophysical properties contain a wealth of information about the properties and processes controlled by and affecting this interface. In addition to ongoing laboratory studies, what we need now are partnerships between geophysicists and geochemists, hydrologists, and biogeochemists to demonstrate, at the field scale, the value of geophysical data for investigating Critical Zone properties and processes related to the solid-water interface in geologic materials.

3.2. Response of NMR Measurements to Solid-Fluid Interfaces in Granular Materials

[40] NMR relaxation measurements provide a way of probing the pore-scale environment of a porous, granular material by observing the relaxation of the pore water following a controlled perturbation in the magnetic field. For water contained in a single, spherical pore, the observed fluid relaxation time constant T_2 is not simply a property of the bulk water but also a reflection of characteristics of the solid-water interface. This is due to the fact that paramagnetic materials at the solid surface enhance the relaxation rate of the hydrogen nuclei in the liquid that contact the solid surface. Provided that diffusion of the nuclei to the surface from all parts of the pore is fast relative to the enhanced relaxation rate at the surface, the exponential relaxation time constant is given by the following expression [*Kleinberg and Horsfield*, 1990]:

$$\frac{1}{T_2} = \frac{1}{T_{2b}} + \frac{1}{T_{2s}} + \frac{1}{T_D}, \tag{12}$$

where T_{2b} is the relaxation time constant of bulk liquid, T_{2s} is the surface relaxation time constant, and T_D is the time constant associated with diffusion of the hydrogen nuclei in an inhomogeneous magnetic field. The link to the solid-fluid interface is found in the following expression for $1/T_{2s}$ [*Senturia and Robinson*, 1970; *Brownstein and Tarr*, 1979]:

$$\frac{1}{T_{2s}} = \rho_2 \frac{S}{V_{\text{pore}}}, \tag{13}$$

where ρ_2 is the surface relaxivity, which is a measure of the extent to which the presence of the solid surface enhances the relaxation of the fluid in the pore space.

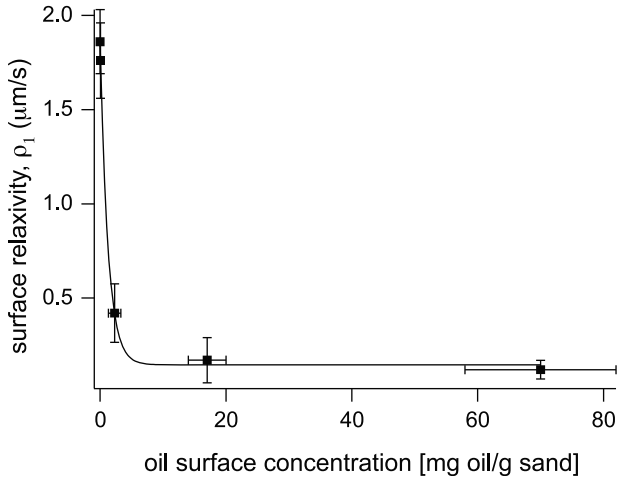

Figure 8. Laboratory NMR relaxation data [from *Bryar and Knight*, 2003] show the marked decrease in surface relaxivity of a quartz sand with the adsorption of oil to the sand surface. The amount of oil, given in terms of the surface concentration, is quantified as the mass of adsorbed oil per gram of sand.

[41] For a distribution of pore sizes there will be a distribution of relaxation times obtained from the NMR data for a water-saturated material. Interpretation of NMR laboratory data commonly utilizes not the full distribution of relaxation times but rather T_{2ML}, the mean log of the T_2 values. The averaged values of the NMR relaxation times of water-saturated sandstones correlate well with the measured permeability. Because T_{2ML}, through its dependence on S/V_{pore}, reflects a volume-averaged pore size, it has been substituted for the hydraulic radius r in the formulations of Kozeny and Carman for permeability, $k \propto r^2\phi$ [*Paterson*, 1983]. Using NMR-derived parameters, the relationship becomes $k \propto (\rho_2 T_{2ML})^2\phi$. This is often altered to the form $k = c(\rho_2 T_{2ML})^2\phi^4$, in which adjustments have been made to accommodate the tortuosity and optimize the fit to experimental data [*Straley et al.*, 1997]; c is an empirically determined constant.

[42] The surface relaxivity, given in equation (13), is influenced by the wettability as well as the paramagnetic content of the solid surface. When a water-wet rock is saturated with a mixture of oil and water, relaxation of the oil (which also contains hydrogen nuclei) can also be measured. Because the oil is prevented from contacting the rock surface by water films, the water relaxation is enhanced but the oil relaxation is not. A reduction in the measured T_2 of oil can be an indication of contact with the surface and wettability changes.

[43] The sensitivity of NMR relaxation times to the size and wettability of the solid surface introduces a potential application of NMR in contaminant hydrology. Laboratory studies have shown the NMR relaxation times to be very sensitive to the adsorption of oil on the surfaces of water-saturated sand grains [*Bryar and Knight*, 2003]. In these studies, relaxation times were found to be affected by changes in the size of the solid-water interface due to adsorption and were also affected by changes in surface relaxivity. The observed reduction in surface relaxivity due to adsorption of small amounts of oil is shown in Figure 8. The mechanism responsible for this reduction is thought to be the physical shielding of the water molecules from the paramagnetic sites on the solid surface due to the presence of the adsorbed oil. The fact that adsorption of such small amounts of oil was found to affect both the dielectric (discussed in section 3.1) and NMR responses suggests that the combination of these measured parameters could be of value for contaminant detection and monitoring their removal.

[44] The surface relaxivity, which describes the capacity of the grain surface to enhance relaxation, generally increases with the concentration of paramagnetic impurities on a surface (e.g., Mn^{2+} or Fe^{3+}) [*Foley et al.*, 1996; *Bryar et al.*, 2000]. Recent studies of water-saturated sands coated with iron-bearing minerals have shown that it is not simply the concentration of Fe^{3+} that determines the surface relaxivity, and thus the relaxation time of the water, but the actual mineralogic form of the iron [*Keating and Knight*, 2007]. In a controlled laboratory experiment, in which columns containing ferrihydrite-coated quartz sand reacted with aqueous Fe(II) solutions, the volume of water relaxing with long relaxation times increased with the formation of goethite and lepidocrocite; a decrease in the average (mean log) relaxation time and a broadening of the relaxation time distribution corresponded to the formation of magnetite [*Keating et al.*, 2008]. These laboratory observations suggest the possible use of NMR to monitor the progress of a geochemical reaction by monitoring the changes in relaxation times due to changes in iron mineralogy. While successfully demonstrated in the laboratory, this now needs to be demonstrated at a field site.

[45] NMR has been used for many years, in many fields of science and engineering, to probe molecular-scale physical and chemical properties. Given the direct link between the measured NMR relaxation time and the size and state of the solid-fluid interface, we are likely to find many new ways of using NMR to characterize processes occurring at and affecting this interface.

4. FLUID-FLUID INTERFACES

[46] Soils, sediments, and rocks in the near-surface region contain a mixture of pore fluids that can include water, air, and other naturally occurring gases and various forms of contaminants (in liquid and gaseous forms). As discussed in section 3, the properties and size of the solid-water interface can have a significant effect on the geophysical properties of geological materials. It is reasonable to ask whether fluid-fluid interfaces can also have an effect on the geophysical properties of a multiphase saturated material.

[47] If we consider two immiscible fluids in a porous medium and assume a condition of thermodynamic equilibrium, the fluids will be distributed in such a way as to

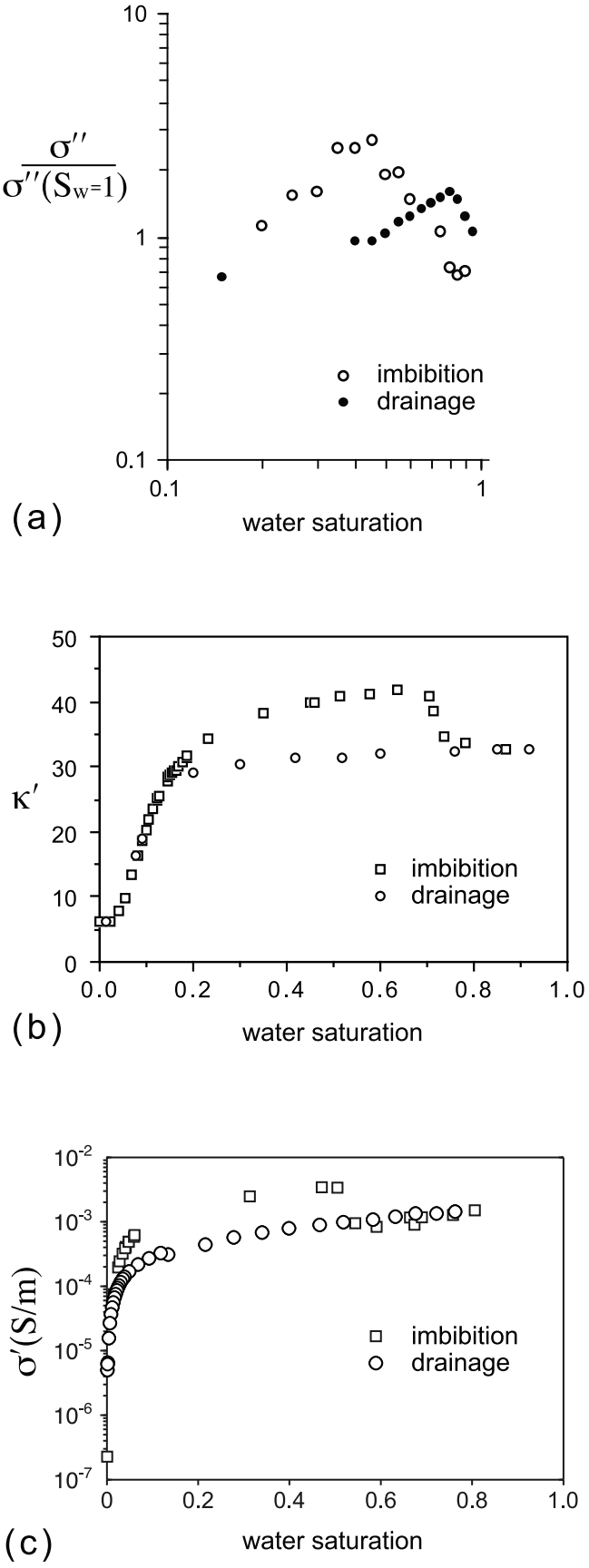

minimize the total interfacial free energy G of the solid-fluid system, where

$$G = \mathrm{IA}_{s/f}\,\gamma_{s/f} + \mathrm{IA}_{f/f}\,\gamma_{f/f}; \tag{14}$$

IA is the interfacial area (i.e., surface area) of the interface, γ is the surface tension of the interface, and the subscripts *s/f* and *f/f* refer to the solid-fluid and fluid-fluid interfaces, respectively. Using a numerical model of a multiphase saturated porous medium, the equilibrium distribution of fluids can be determined by minimizing G [*Knight et al.*, 1990; *Silverstein and Fort*, 2000], and the size of the fluid-fluid interface ($\mathrm{IA}_{f/f}$) can be calculated [*Silverstein and Fort*, 2000]. It is highly unlikely, however, that fluids in the near surface will be found in this equilibrium state. The various processes associated with increasing and decreasing water content and with the movement and degradation of contaminants will lead to many varied pore-scale fluid distributions. A key point, for the purposes of this review, is the fact that these various distributions of pore fluids can correspond to significant variations in the fluid-fluid interfacial area; these changes in fluid-fluid interfacial area have been documented by the use of interfacial tracers [*Jain et al.*, 2003]. In our review we discuss the response seen in the measured geophysical response of multiphase-saturated materials to changes in fluid distribution. These results cannot be explained by accounting only for the volumes of fluids present and suggest that geophysical properties could also be used to quantify, or monitor changes in, fluid distribution or fluid-fluid interfacial area.

4.1. Response of Electrical Measurements to Fluid-Fluid Interfaces in Granular Materials

[48] The concept of an electrical potential at fluid-fluid interfaces is well established in surface science but, surprisingly, is rarely considered in the interpretation of geophysical data. In this section we review laboratory data that have been interpreted as revealing a dependence of electrical properties on the size of the fluid-fluid interface.

[49] In Figure 9 are shown the measured changes in electrical properties as water saturation was increased (imbibition) and decreased (drainage). Shown, as a function of water saturation, are the laboratory measurements of σ'' of a sand at 1 Hz [from *Ulrich and Slater*, 2004], κ' of a sandstone at 500 kHz (data from *Knight and Nur* [1987b]), and σ' of a sandstone at 500 kHz (data from *Knight* [1991]). In all cases we see saturation-related hysteresis with a maximum in σ'', κ', and σ' at an intermediate saturation during imbibition. The behavior of all three properties can

Figure 9. The measured changes in electrical properties as water saturation was changed by imbibition (increasing saturation) and drainage (decreasing saturation): (a) σ'' of a sand at 1 Hz [from *Ulrich and Slater*, 2004], (b) κ' of a sandstone at 500 kHz (data from *Knight and Nur* [1987b]), and (c) σ' of a sandstone at 500 kHz (data from *Knight* [1991]).

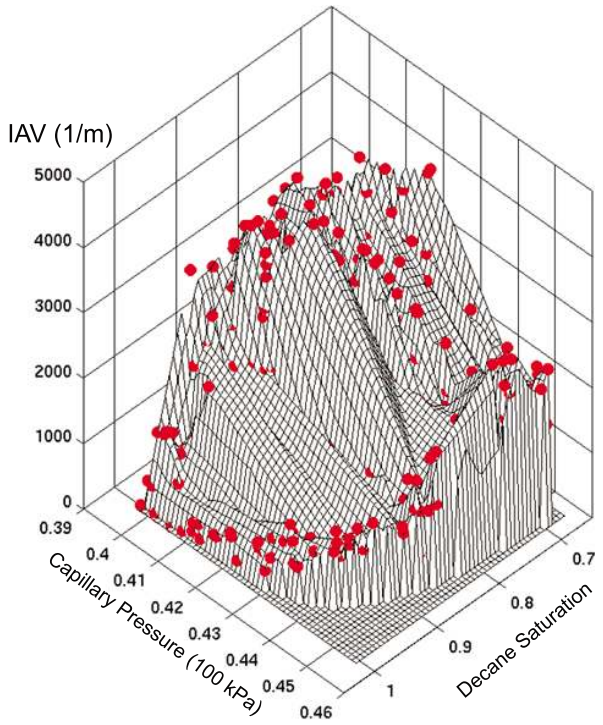

Figure 10. The interfacial area per volume (IAV) between nonwetting and wetting fluids as a function of capillary pressure and decane saturation [*Cheng et al.*, 2004].

be explained with a simple model of pore-scale fluid distribution where the key factor is the size of the continuous fluid-fluid, i.e., air-water, interface with its associated surface conductivity and charge polarization. The proposed model suggests that processes involved during imbibition tend to develop thin connected air pockets, while drainage tends to lead to segregation of fluids. The air-water interface will be much larger in the former case.

[50] The hysteresis observed in electrical properties is strikingly similar to that seen in the relationship between capillary pressure P_c and fluid saturation S_f. This relationship is typically hysteretic, with values of P_c measured during imbibition being different from those measured during drainage. Laboratory data [*Cheng et al.*, 2004; *Chen et al.*, 2007] from micromodels demonstrated that accounting for the interfacial area per volume (IAV) between nonwetting and wetting fluids can remove the hysteresis in the relationship between P_c and saturation S_f in porous media. Figure 10 shows IAV as a function of capillary pressure and saturation. Although each 2-D projection of the surface is hysteretic, for a given degeneracy between two data points in P_c and S_f, the IAV differentiates between them.

[51] Accounting for IAV removes the hysteresis in the relationship between P_c and fluid saturation. Could accounting for IAV also remove the hysteresis in the relationships between electrical conductivity and dielectric constant and fluid saturation? If so, this would be a first step toward estimating IAV from the measurement of electrical properties.

[52] Further laboratory and theoretical studies are needed to determine the properties of fluid-fluid interfaces and to then develop a fundamental understanding of how these properties, the sizes of the fluid-fluid interfaces, and the related pore-scale distribution of fluids all contribute to the electrical properties of granular materials. There is also a need for controlled field experiments designed specifically to determine whether the behavior being observed in laboratory data can be detected in the field. This is a fruitful area of future research, investigating the use of geophysical measurements to acquire information not simply about the *volume* of pore fluids in a subsurface region but about the *distribution* of pore fluids, critical information for understanding and predicting a wide range of hydrologic and geochemical processes.

4.2. Response of Seismic Measurements to Fluid-Fluid Interfaces in Granular Materials

[53] Despite the fact that the seismic properties of a material have no direct relationship to the electrical properties of a material, they exhibit a strikingly similar form of hysteresis in their dependence on fluid saturation. In Figure 11 we show saturation hysteresis in data [from *Knight and Nolen-Hoeksema*, 1990] for the *P* wave velocity of a tight gas sandstone measured as water saturation was first increased (imbibition) and then decreased (drainage). The form of the data was attributed to changes in the geometry of the water and air phases. It was proposed that the extended gas pockets during imbibition reduced the bulk modulus of the pore space and resulted in lower elastic wave velocities. For multiphase flow in a porous medium, accounting for IAV lifted the ambiguity in the capillary pressure-saturation relationship because IAV quantifies the spatial distribution of the fluid phases [*Cheng et al.*, 2004; *Chen et al.*, 2007]. An outstanding question is whether IAV may play a role in affecting seismic wave propagation in a porous medium containing two fluid phases. If so, it might

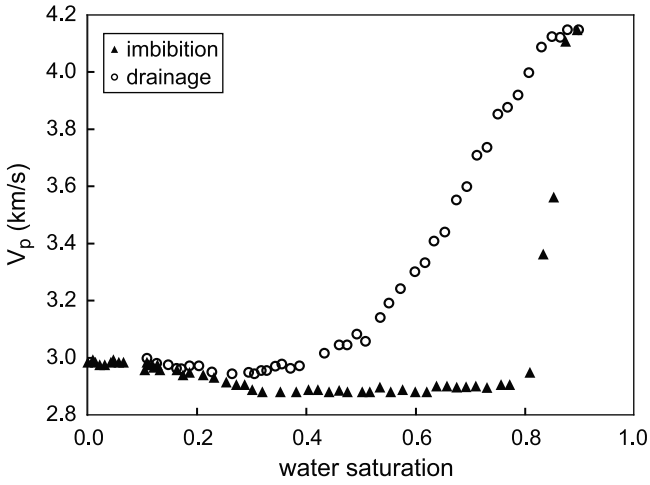

Figure 11. *P* wave velocity of a tight gas sandstone measured as water saturation changed through imbibition and drainage (data from *Knight and Nolen-Hoeksema* [1990]).

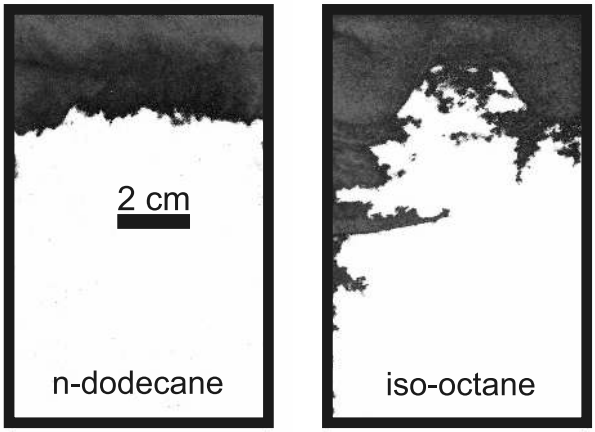

Figure 12. Photographs from a set of experiments designed to explore the effect of fluid-fluid interfaces on seismic properties [from *Seifert et al.*, 1998]. In the experiments, *n*-dodecane and iso-octane were injected into the top of a water-saturated sand pack contained between glass plates, displacing water out the bottom. Note the different geometry of the displacement front for the two fluids.

be possible to find ways of using a combination of electrical and seismic properties to extract information about the size and the properties of the fluid-fluid interface.

[54] Figure 12 contains photographs [from *Seifert et al.*, 1998] from a set of experiments designed to explore the effect of larger-scale fluid-fluid interfaces on seismic properties. In these laboratory column experiments, *Geller and Myer* [1995] injected two nonaqueous phase liquids (NAPLs), *n*-dodecane and iso-octane, into the top of a water-saturated sand pack, displacing water out the bottom, while measurements were made of *P* wave velocity and the amplitude of the received wave; the waves propagated from the top to the bottom of the sand pack. The data points for 100% NAPL saturation were measured in separate sand packs. The central frequency of the transmitted waves ranged from 300 to 400 kHz, resulting in wavelengths from 0.3 to 0.6 cm over the observed velocity range. As can be seen in Figure 12 the interface between the NAPL-saturated region and the water-saturated region was quite different for the two fluids. The higher viscosity of *n*-dodecane, relative to water, resulted in a stable displacement front. The viscosity of iso-octane is less than that of water, which resulted in viscous fingering of the NAPL into the water-saturated areas. This fingering led to bypassing of patches of water-saturated regions that remained trapped behind the displacement front.

[55] The *P* wave velocity for both NAPLs, shown in Figure 13a, was found to decrease almost linearly as NAPL saturation increases (and water saturation decreases). This dependence of velocity on saturation simply reflects the change in the volume fractions and the different velocities of the two fluids; the NAPLs have a lower velocity than that of water. The amplitude data (presented as measured amplitude A normalized by the amplitude in the water-saturated sand A_{max}), shown in Figure 13b, however, are more complex in form. While the amplitude for *n*-dodecane decreases monotonically with NAPL saturation, the amplitude data for iso-octane do not show a simple dependence on saturation. This difference in the measured responses for the two NAPLs is attributed to the geometry of the fluid-fluid interfaces, or displacement fronts, for the two fluids, shown in the photographs in Figure 12. The scale of the photographs shows that the viscous fingers that form as iso-octane displaces water are several centimeters in length, which is greater than the 0.5 cm wavelengths of the *P* wave through the sample. For these length scales, it is likely that the *P* wave energy is scattered at the NAPL-water interfaces, so the amplitude responds to the structure of the fluid-fluid interface.

[56] Field data are typically acquired at much lower frequencies than laboratory data, which result in longer wavelengths, likely to be sensitive to larger-scale heterogeneity. A key question, therefore, is whether the same effect would be seen when measurements were made at lower frequencies. To address this question, an experiment was performed in a tank, 60 cm in diameter and 75 cm high, using 90 kHz

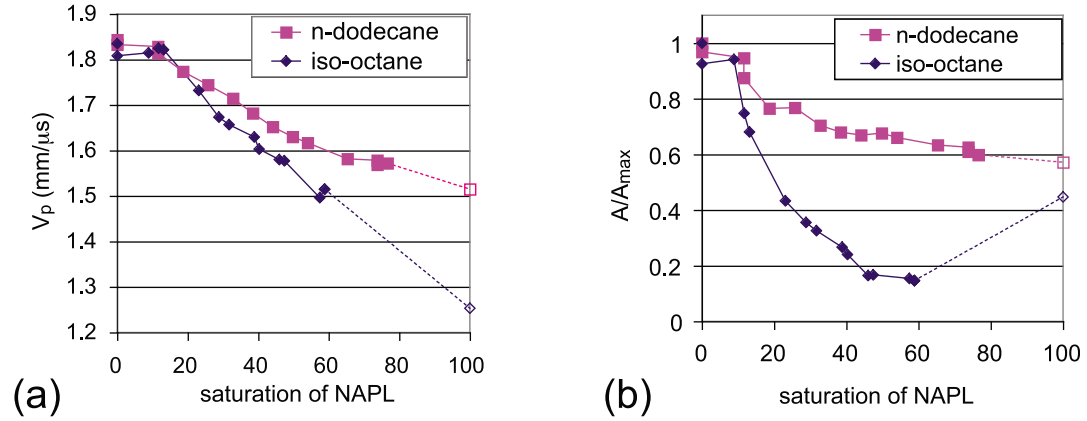

Figure 13. The *P* wave (a) velocity and (b) amplitude data (presented as measured amplitude A normalized by the amplitude in the water-saturated sand A_{max}) for *n*-dodecane and iso-octane as a function of NAPL saturation in a sand column. Reprinted from *Geller and Myer* [1995], copyright 1995, with permission from Elsevier.

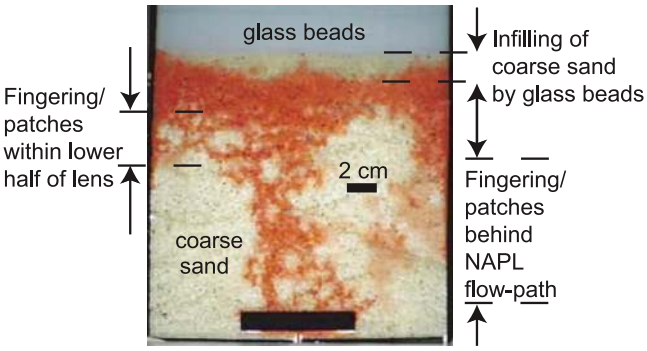

Figure 14. Photograph of dyed *n*-dodecane, which was injected into the bottom of a mixture of glass beads/sand contained between two glass plates, flowed upward, and formed a lens at the bottom of the glass bead layer. The photograph shows the infilling of the coarse sand by the glass beads and the NAPL distribution within the lens.

P waves with wavelengths on the order of 2 cm [*Geller et al.*, 2000]. The bottom two thirds of the tank was packed with coarse quartz sand, over which a layer of fine glass beads formed a capillary barrier; *n*-dodecane was injected from the bottom of the water-saturated tank, while the *P* wave source and receiver were moved over the depth of the tank through acrylic tubes located at opposite sides of the tank. When the *P* wave source and receiver were aligned (at the same depth in the tank), the received waveforms represent horizontally averaged properties; this arrangement is referred to as "zero offset."

[57] Photographs of dyed *n*-dodecane in the same system, but between glass plates, were used in the interpretation of the data. The NAPL, injected into the bottom of the plates, flowed upward and formed a lens at the bottom of the glass bead layer. The photograph in Figure 14 shows the infilling of the coarse sand by the glass beads and the NAPL distribution within the lens. The NAPL saturation decreased with depth through the lens, and the NAPL distribution became more patchy toward the bottom of the lens.

[58] The records of the waveforms before and after NAPL injection into the cylindrical tank are displayed in Figures 15a and 15b and show a change in the amplitude of the first arrival *P* wave (shown as gray scale intensity). The reference zero-offset data, obtained when the tank was saturated with water, shows attenuation and diffraction due to the glass bead–sand interface. This interface is not sharp and includes a transitional region, indicated by the pair of dashed black lines in Figure 15, of about 2–3 cm where the smaller diameter beads fill the pore space of the underlying coarse sand. A comparison of the postinjection scan (Figure 15b) to the reference scan (Figure 15a) shows delayed traveltimes and amplitude reductions of 60%–95% in the 15 cm below the glass bead layer due to the presence of the NAPL lens. The highly attenuated first arrivals within the lens are indicated by a dashed white line. Below the lens, the residual NAPL causes amplitude reductions of 1%–30% and changes in diffraction patterns.

[59] In both the column and tank experiments, as NAPL displaced water, velocity was found to depend on volume fractions and bulk properties of the fluid and solid phases, whereas attenuation was found to be very sensitive to the geometry of the fluid-fluid interface. The irregular and patchy NAPL-water distribution formed by channelized flow was interpreted as causing increased attenuation due to scattering. This form of attenuation is likely to be sensitive to the geometry of the scattering volumes. The hope is that further laboratory and theoretical studies will lead to an improved understanding of the relationship between measured seismic properties and the geometry and area of the interface at the displacement front between immiscible fluids. The challenge, again, will be to conduct the upscaled field experiments to determine whether the same seismic

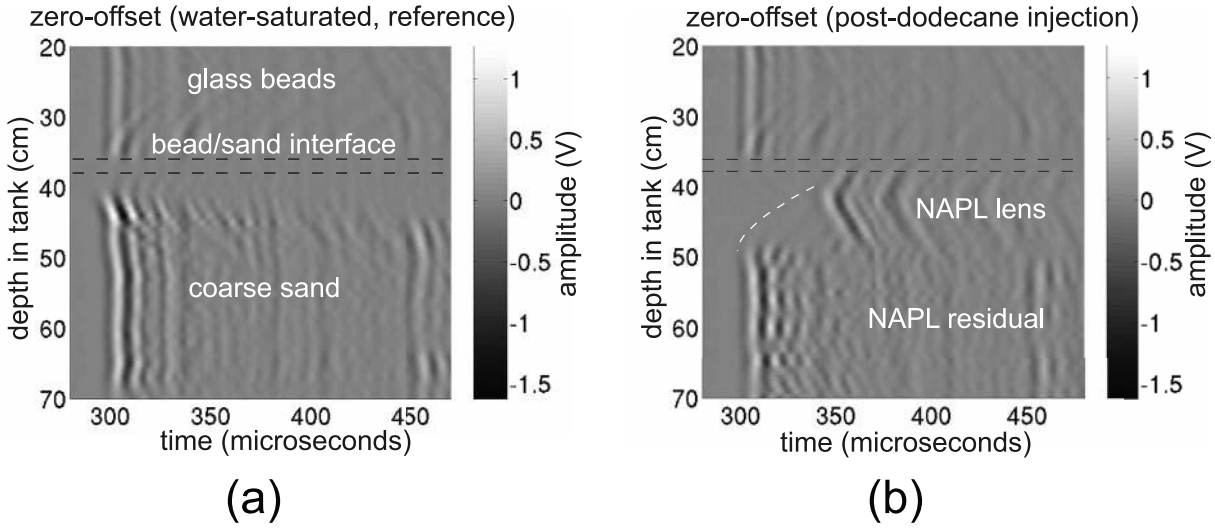

Figure 15. The records of seismic waveforms (a) before and (b) after NAPL injection into a cylindrical tank [*Geller et al.*, 2000].

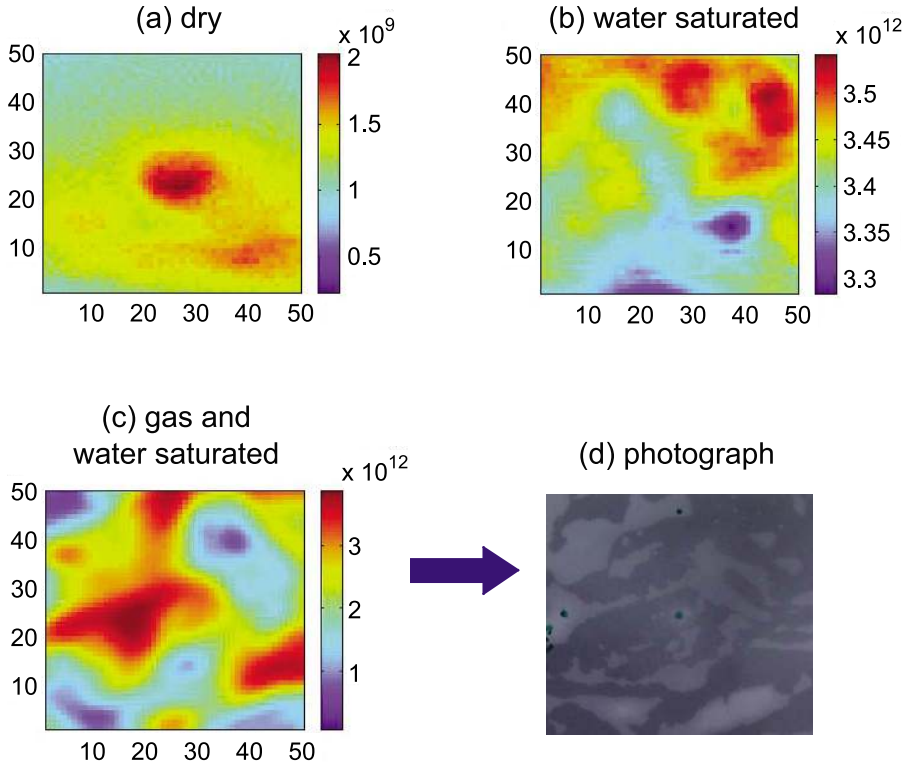

Figure 16. The predicted fracture specific stiffness from acoustic imaging experiments for a synthetic fracture in lucite for the following conditions: (a) dry, (b) fully water saturated, and (c) saturated with a mix of gas and water. (d) Digital photograph showing the distribution of the gas and water for the case in Figure 16c. In Figure 16d, the light gray regions represent gas, and the dark gray regions represent water.

response exists at the field scale, where the length scale of fluid phase heterogeneities relative to the propagating wavelength is unknown. If so, this could provide an important link from seismic data to properties governing subsurface flow and transport.

4.3. Response of Seismic Measurements to Fluid-Fluid Interfaces in Fractures

[60] The void space within a fracture can be filled with multiple fluid phases. As with granular materials, the interfaces between the fluids can affect seismic measurements but in a way that provides a more direct link between the fluid-fluid interfaces and the measured geophysical property. The interface between two fluid phases will affect fracture specific stiffness because the fluid-fluid interfaces form "bridges" between the two fracture surfaces. The effect on the fracture stiffness is a function of the surface tension of the fluid-fluid interface and the length of the bridge.

[61] The work of *Moerig* [1996] investigates this phenomenon. In their study, the seismic attenuation of synthetic cracks saturated with a liquid and a gas was measured. They observed that reductions in surface tension between the fluid phases increased the seismic attenuation. The increase in attenuation was attributed to a reduction in the stiffness of the membrane formed by the liquid-gas interface. This membrane is sensitive to a surface tension determined by the two fluid phases and the solid phase in contact with the fluids. A high surface tension can stiffen a crack and also inhibit the complete release of pressure built up in the fluid during deformation from a passing wave. For a fracture, the number of membranes made by fluid-fluid interfaces between the two fracture surfaces will affect fracture stiffness. Thus, IAV, which is a pore-scale length scale, can affect macroscopic measurements of seismic wave attenuation and velocity.

[62] *Xian et al.* [2002] made acoustic measurements on a fracture saturated with gas and water (Figures 16c and 16d) and predicted fracture stiffness. The gas-filled regions of the fracture correspond approximately to lower values of fracture stiffness than the water-filled regions. The observed variation in fracture stiffness does not match the fracture heterogeneity for the fracture in the dry or fully water-saturated condition (Figures 16a and 16b). The heterogeneous distribution of gas and water plays a stronger role in controlling the transmission of energy across the fracture than the contact area. For all locations, the fracture specific stiffness is greater for the waves propagated across the fracture when saturated with gas and water than when dry.

[63] While more experimental and theoretical work is required to fully understand the way in which fluid-fluid interfaces in fractures contribute to fracture stiffness, this study suggests that additional research will enable us to quantify the effect of fluid-fluid interface spatial distributions and the

surface tension of these interfaces on seismic wave propagation across fractures.

5. SOLID-SOLID INTERFACE

[64] The solid-solid interface, made up of the contacts between grains and across fractures, controls the mechanical properties of geological materials as well as the hydraulic properties of the material by affecting the connectivity and tortuosity of the void space. In reviewing the laboratory data showing the link between the state of the solid-solid interface and geophysical properties, we find that only seismic properties have been shown to be sensitive to the size and state of this interface.

5.1. Response of Seismic Measurements to Solid-Solid Interfaces in Granular Materials

[65] There are two key factors related to the grain contacts that have a direct impact on the mechanical and hydraulic properties of the material: the effective stress acting on the contacts and the nature of the material filling or surrounding the contact areas. The seismic response of a material is very sensitive to both of these factors, suggesting that seismic data can be used to obtain information that is needed to characterize in situ mechanical and hydraulic properties.

[66] The role of effective stress in determining grain-to-grain contact stiffness, and thus seismic properties, has been studied both theoretically and experimentally for systems ranging from suspensions to granular solids. We can gain insights into the relationship between seismic wave velocities and attenuation and the effective stress at grain contacts by describing laboratory observations that have been made of a solid-fluid system as it changed from a suspension to a solid. These observations demonstrate the difference in the effect that solid-fluid and solid-solid interfaces have on wave propagation through geologic material. Starting with a suspension (i.e., solid-fluid interfaces), which typically corresponds to a porosity value above ~40%, only *P* waves can be transmitted; the system has no rigidity or shear structure, so *S* waves cannot be transmitted. As the grains move closer together (but are not yet in contact), hydrodynamic coupling between the grains starts to take effect. The resulting increase in velocity is generally small at this stage. In contrast, in experiments conducted by *Green and Esquivel-Sirvent* [1999] on kaolinite particles suspensions, a peak in *P* wave attenuation was observed at the point interpreted as corresponding to the transition from a suspension (solid-fluid interfaces dominate) to a fluid-saturated granular solid with finite rigidity (solid-solid interfaces dominate). Because the hydrodynamic coupling depends on the fluid viscosity, the magnitude of the attenuation and the grain concentration at which the peak attenuation occurs are frequency dependent. This anomalous attenuation diminishes as the separation distance between the grains becomes much less than the viscous skin depth, and then the suspension transitions to a solid by gaining rigidity.

[67] After the transition to a solid occurs by the formation of solid-solid interfaces from the establishment of a grain-supported framework, the seismic wave velocities are strongly dependent on the conditions at the grain contacts. When these contacts are initially formed (e.g., at very low effective stress), the contact mechanics are determined by the surface energy considerations; this can be seen in the laboratory data of *Clark et al.* [1980], where surface energy conditions were varied. As effective stress increases and contacts stiffen, surface energy is no longer a dominant factor, but solid-solid interfacial effects continue to impact the elastic wave velocities through the generation of new grain contacts. Experiments have shown that during the early stages of consolidation, the amplitude of the *P* wave typically shows an initial decrease and then increases at a level of stress that depends on the frequency and grain size. This behavior has been observed not only in the laboratory using ultrasonic waves but also in oil and gas reservoirs at much lower frequencies (A. Cheng, personal communication, 1998).

[68] A possible explanation for the dependence of attenuation on effective stress is the link between effective stress and the spatial variation in stiffness in a material. A number of theoretical models have been developed to describe attenuation in a porous, fluid-filled material when there is spatial heterogeneity in terms of the stiffness of the material [e.g., *Dvorkin et al.*, 1995; *Endres*, 1998; *Chapman et al.*, 2002; *Taylor and Knight*, 2003; *Pride et al.*, 2004]; these models treat the case where the elastic wavelength is much greater than the scale of the heterogeneity in stiffness. Such models may explain the observed changes in the amplitude of the *P* wave, if the concept of "stress chains" is used to represent the stiffness heterogeneity. A stress chain is defined as a skeletal structure of load-bearing grains within a random packing of grains under confining stress [e.g., *Liu et al.*, 1995]. Because the load between the grains increases the contact stiffness, the stiffness of the medium will be much higher within a stress chain than in the surrounding grains. The passage of a seismic wave induces differences in pore pressure between the stiff skeletons and softer, more compliant regions. For the pore pressure to reequilibrate during the passage of the seismic wave, diffusion must occur over a length scale comparable to that of the stiffness heterogeneity. If this occurs, there is a maximum in viscous energy loss and large attenuation of the seismic energy. This theoretical model, along with the laboratory observations, suggests that seismic monitoring could be used to detect or monitor the critical transition from a suspension to a load-bearing solid (e.g., from uncompacted to compacted sediments) or to detect the loss of cohesion as a load-bearing solid becomes a suspension. The latter could be an application of great importance in monitoring the onset of liquefaction or failure in granular materials.

[69] The effect of material at grain contacts on elastic wave velocities has been assessed through both experimental and theoretical studies. *Dvorkin et al.* [1991, 1994] showed that the amount of cement is more important than the stiffness of the cement in determining elastic properties; even small volumes of cement at grain contacts act to increase a rock's elastic moduli and thus the elastic wave

velocities. A similar response to grain contact alteration was observed by *X. Li et al.* [2001] for residual hydrocarbon distributed within an unconsolidated water-saturated sediment. *X. Li et al.* [2001] noted a correlation between the microscopic morphology of the grain-hydrocarbon interface and the velocity and attenuation determined from the seismic waveforms. Hydrocarbon bridging at the grain contacts was found to increase the velocity and decrease attenuation. Alternatively, when only filaments of wax occurred on the grains, velocity decreased and attenuation increased. In these experiments, seismic wave attenuation was found to be sensitive to alteration of the grain contact stiffness at levels of hydrocarbon saturation as low as a few percent (1%–3%) and sensitive to spatial features (bridging between grains) that were ~1/100 of a wavelength.

[70] Alteration of grain contacts also occurs because of biological activity. Recently, *DeJong et al.* [2006] demonstrated that the shear stiffness of a sand can be enhanced and improved through microbial activity. They used the microbe *Bacillus pasteurii* to induce calcite precipitation in an unconsolidated sand and to monitor the change in the shear properties of the sand using a bender element technique [*Landon*, 2004]. Relative to the initial condition of the sand, the shear wave velocity of the sand doubled in magnitude during the treatment period. The microbially induced cement was observed on grain surfaces and at grain contacts. In a later paper, *DeJong et al.* [2010] noted that enhancement of the strength and stiffness of soil from microbial processes requires that some of the precipitated biominerals form at grain contacts rather than just coating the grains; that is, the condition of the solid-solid interface dominates the shear response of the sand.

[71] The response of seismic properties to the level of effective stress at grain contacts and to the microscopic interface morphology illustrates the complicated nature of the dependence of macroscopic seismic properties on micromechanics. These studies demonstrate that changes to grain contacts through time-dependent processes result in changes in the seismic properties of granular media. Given that changes to grain contacts will also impact the mechanical and hydraulic properties, this suggests another way in which geophysical data, through a sensitivity to solid-solid interfaces, can be used to obtain information about Critical Zone properties.

5.2. Response of Seismic Measurements to Solid-Solid Interfaces in Fractures

[72] In granular materials, the stiffness of the grain contacts (the solid-solid interfaces) affects the seismic response of the material. In fractured materials, the fracture stiffness affects the seismic response. Fracture stiffness has its origins in the microscale heterogeneity of the solid surfaces in contact, with fracture specific stiffness determined by the amount and spatial distribution of the solid-solid contact area and by the size (aperture) and spatial distribution of the void space [*Brown and Scholz*, 1985, 1986; *Hopkins et al.*, 1987; *Hopkins*, 1990]. For granular materials we considered the way in which stress and cementing material at the solid-solid contacts affect seismic properties. For fractured materials we consider these same two factors.

[73] When a normal or shear stress is applied to a fracture, the contact area and the aperture distributions will change, resulting in an increase in fracture specific stiffness. Assuming a fracture can be represented as a nonwelded contact [*Mindlin*, 1958; *Kendall and Tabor*, 1971; *Murty*, 1975; *Schoenberg*, 1980, 1983; *Kitsunezaki*, 1983; *Pyrak-Nolte et al.*, 1990], an increase in fracture stiffness affects the transmission of seismic waves, the amplitude of reflected energy, the group time delay, and also the frequency content of the signal. These effects on seismic wave propagation suggest that the frequency-dependent transmission and reflection of both *P* and *S* waves can be used to monitor changes in fracture specific stiffness caused by changes in stress, fluid content, and reactive flow [*Chen et al.*, 1993; *Pyrak-Nolte et al.*, 1996; *Suarez-Rivera*, 1992; *Nakagawa and Schoenberg*, 2007; *Acosta-Colon et al.*, 2009]. Of specific interest for near-surface applications is the fact that the stress on the fracture will also change the mechanical and hydraulic properties of the fracture. This suggests that seismic measurements could be used, indirectly, to monitor changes in these key properties that control many subsurface processes [*Pyrak-Nolte and Morris*, 2000].

[74] No research has been conducted to determine if transmitted and/or reflected seismic waves can distinguish the stress state (e.g., single mode versus mixed modes) on a fracture. However, *Nakagawa et al.* [2000] showed that certain converted modes from a fracture are directly linked to the presence of static shear stress on a fracture. Laboratory experiments have shown that a statically sheared rough fracture can convert normally incident plane *P* waves into *S* waves and *S* waves into *P* waves, with the direction of *S* wave particle motion indicating the direction of the static shear and the amplitude increasing with increasing shear stress. This anomalous conversion of seismic waves arises because the deviation of the normals of the local contact area from the normal to fracture plane are biased by the application of shear stress. This results in anisotropic scattering of the high-frequency components of the incident wave from the open voids and contacting asperities. The scattering generates both *P* and *S* waves that constructively interfere to generate coherent, converted plane waves.

[75] Though the state of stress on a fracture may be hard to determine, *Oliger et al.* [2003] showed in laboratory experiments that stress gradients along a fracture can complicate the interpretation of fracture specific stiffness from seismic measurements. They showed that a single planar fracture with a radial stress gradient (fracture specific stiffness that is low in the center of the fracture and increases along the radius) behaves as a seismic lens that focuses seismic energy to a beam waist at a focal plane. Whether a diverging or converging wavefront is measured depends on the location of the measurement relative to the focal plane. *Pyrak-Nolte* [2007] noted that a linear gradient in fracture specific stiffness will cause a wavefront that is normally incident on the fracture to refract because the time delay caused by the fracture depends on fracture specific

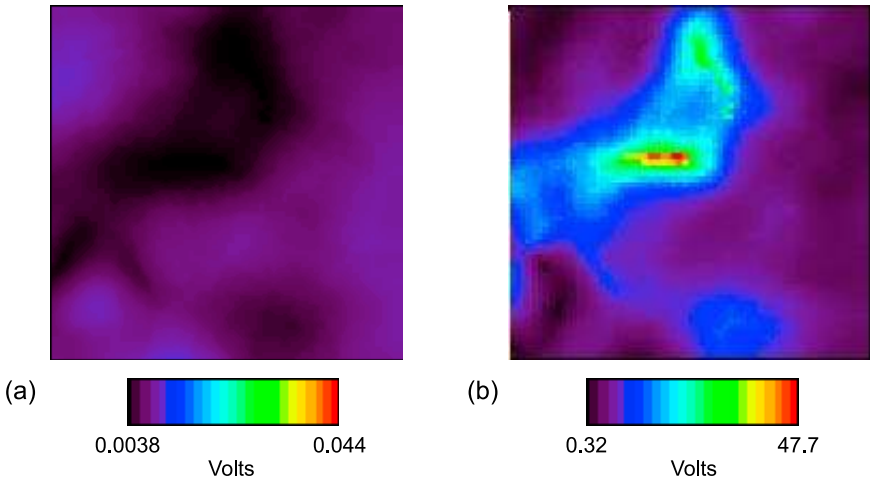

Figure 17. (a) Acoustic signal amplitude transmitted through a single water-saturated fracture in granite prior to chemical invasion. (b) The fractional relative amplitude 32 days after chemical invasion into the fracture (after *Gilbert and Pyrak-Nolte* [2004], with permission from the American Rock Mechanics Association).

stiffness. High fracture specific stiffness produces a smaller time delay than a low fracture specific stiffness. Thus, knowledge of the state of stress on a fracture is crucial to correct interpretation of seismic wave attenuation and velocity in both laboratory and field investigations [*Hildyard and Young*, 2002].

[76] In addition to stress affecting fracture specific stiffness, geochemical processes such as dissolution and precipitation also affect fracture stiffness [*Gilbert and Pyrak-Nolte*, 2004; *Acosta-Colon et al.*, 2009]. Mineral dissolution in a fracture weakens and erodes the contact area in the fracture and widens the apertures [*Detwiler*, 2008], which causes a reduction in fracture specific stiffness and seismic velocities, and an increase in attenuation. On the other hand, mineral deposition in a fracture tends to reduce apertures and increase contact between the fracture surfaces [*Singurindy and Berkowitz*, 2005], both of which lead to an increase in the stiffness of a fracture as well as a reduction in permeability and cause a corresponding increase in the amplitude and velocity of seismic waves transmitted across the fracture. Figure 17 shows acoustic images of a water-saturated fracture in granite, prior to mineral deposition, and the relative acoustic amplitude 32 days after mineral deposition. The increase in amplitudes indicated that mineralization had stiffened the fracture. The most reliable indicator of mineral deposition was found to be a narrowing of the distribution of the frequency content of the acoustic data [*Gilbert and Pyrak-Nolte*, 2004]. The narrowing of the distribution indicated that mineral deposition in the fracture homogenized the fracture stiffness.

[77] If seismic data can be used to monitor mineral deposition in fractures, the data could also be used to monitor, indirectly, the associated changes in hydraulic properties. The largest relative change in acoustic amplitude, seen in Figure 17, occurred in regions of the fracture that originally exhibited low amplitudes and high attenuation of the acoustic signal, showing that mineralization had preferentially occurred in the regions with large initial apertures and low fracture stiffness. These regions were also initially the dominant flow paths. The mineralization stiffened the fracture either by a reduction in aperture or an increase in contact area, both of which would act to reduce hydraulic conductivity.

[78] In summary, laboratory observations suggest that seismic data could be used to obtain critical information about the properties of the solid-solid interfaces in fractured materials that govern the movement of fluids and related geochemical and biogeochemical processes. We conclude this section, as in others, by noting that field experiments need to be conducted to determine whether the response of seismic measurements to fracture properties seen in the laboratory could also be detected in the field.

6. FIELD-SCALE MEASUREMENTS AND APPLICATIONS

[79] The focus of this paper is a review of laboratory studies of the geophysical properties of granular and fractured media, illustrating the links found between the magnitude of these properties and the properties of solid-fluid, fluid-fluid, and solid-solid interfaces. Throughout the paper we comment on the potential to use these laboratory-scale findings to develop new ways of using geophysical methods at the field scale for studying Critical Zone properties and processes. In this section we consider field-scale measurements and applications and ask the following questions: (1) To what extent have we been able to use field-based geophysical methods to study solid-fluid, fluid-fluid, and solid-solid interfaces in the Critical Zone? (2) What are the current challenges we face in using field-based geophysical methods for studies of the Critical Zone?

TABLE 1. Six Examples of Surface-Based Geophysical Methods Used for Near-Surface Applications[a]

Surface-Based Geophysical Method	Lateral Extent of Surveyed Region	Depth of Surveyed Region	Resolution of Measurement	Acquired Data	Geophysical Properties of Interest
Electrical resistivity	meters to hundreds of meters	meters to ~100 m	~0.5 m to meters	electrical potential generated by transmission of current	DC conductivity (σ_{DC})
Ground-penetrating radar	meters to hundreds of meters	meters to tens of meters	tens of centimeters to meters	amplitude and arrival time of reflected electromagnetic energy	dielectric constant (κ') at antenna frequency (between 1 MHz and 1 GHz)
Induced polarization	meters to hundreds of meters	meters to ~100 m	~0.5 m to meters	decay in electrical potential following current pulse and frequency dependence of complex impedance	imaginary part of the complex electrical conductivity (σ'') at frequencies from mHz to kHz
Surface nuclear magnetic resonance	tens to hundreds of meters	~50 m to ~100 m	meters	decay in nuclear magnetization following radio frequency pulse	relaxation time constant
Seismic reflection	tens to hundreds of meters	meters to ~100 m	meters	amplitude and arrival time of reflected elastic energy	elastic wave velocities and attenuation
Spontaneous potential	meters to hundreds of meters	meters to ~100 m	~0.5 m to meters	naturally occurring electrical potential, i.e., self-potential	electrochemical potential, redox potential, and streaming potential

[a]The lateral extent and depth of the surveyed region and resolution of the measurement are all typical values for near-surface applications. Near surface is defined as the top ~100 m of Earth, so the maximum depth given is limited to ~100 m for all methods. The listed geophysical properties of interest are the focus of this paper and are obtained through processing and/or inversion of the acquired data.

6.1. Geophysical Field Measurements: Surface-Based Methods

[80] We have reviewed laboratory studies of electrical properties, NMR relaxation time constants, and seismic properties, highlighting the relationships between these properties and the solid-fluid, fluid-fluid, and solid-solid interfaces in geological materials. In order to observe and use these relationships in studies of the Critical Zone, we need to (1) make the geophysical field measurement to acquire the data, (2) analyze the acquired data to obtain the geophysical property of interest, and (3) interpret the geophysical property to extract the information needed about the interfaces.

[81] Table 1 lists the surface-based (i.e., deployed at Earth's surface) geophysical methods that can be used to obtain information about the electrical properties, NMR relaxation time constants, and seismic properties for near-surface applications. Most of these methods are used in a wide range of applications, from monitoring changes in soil moisture at a scale of tens of centimeters to imaging deep crustal structure. Choices are made during data acquisition that optimize the sampling of the region of interest in the field survey. These choices, such as the type and spacing of the geophysical sensors, typically involve trade-offs between the spatial resolution that can be achieved with the measurement and the extent (lateral and depth) of the surveyed region. Given that the focus of this paper is on studying the Critical Zone in the upper ~100 m of the subsurface, we have provided in Table 1 estimates of survey extent and resolution relevant for applications that involve measurement within that region. Given in Table 1 are the forms of the acquired data and the geophysical properties obtained through analysis of the data. We note that many of the geophysical properties listed in Table 1 can also be obtained with measurements made using borehole methods. We have limited ourselves to discussion of surface-based methods as these provide fully noninvasive means of subsurface imaging.

[82] The specific issue of interest in this review is whether or not we can use geophysical field methods to obtain information about interfaces. In section 6.2 we describe field-scale studies in which geophysical methods have been used to acquire information about pore-scale interfaces, building on the laboratory studies discussed in this review. In section 6.3, we then describe field-scale studies in which geophysical methods have been used to acquire information about field-scale interfaces. We conclude in section 6.4 by discussing the challenges of acquiring and interpreting geophysical data for Critical Zone applications.

6.2. Geophysical Field-Scale Imaging of Pore-Scale Interfaces

[83] Recent work has begun to take the laboratory-scale observations of the link between electrical properties and S/V_{pore} to the field scale and to investigate how measurement of σ'' with induced polarization (IP) field measurements could be used to map out the spatial variation in K at a field site [*Slater and Glaser*, 2003; *Kemna et al.*, 2004; *Hördt et al.*, 2007]. One approach is to use the measurement of σ'' to estimate S/V_{pore}, which is then used in a Kozeny-Carman type of expression for the field-scale characterization of hydraulic conductivity. This was the approach taken by *Slater and Glaser* [2003], who used IP measurements to generate an image of hydraulic conductivity distribution between two 15 m deep wells spaced 10 m apart in an alluvial aquifer of the Kansas River floodplain. Obtaining in situ estimates of K or k noninvasively using geophysical

methods would provide information that is essential in many studies of processes occurring in the Critical Zone.

[84] The link between electrical properties, measured at low frequencies, and the surface area of metallic grains has been very successfully exploited in mineral exploration IP measurements. There is now growing interest in using IP measurements to obtain information about the electrochemistry of environmental processes involving metals. The IP method could provide a means of investigating the performance of Fe_0-based permeable reactive barrier technologies during remediation of contaminated groundwater [*Slater et al.*, 2005]. Through such applications, geophysical measurements could play a central role in the design and monitoring of the remediation of contaminated sites. The IP method provides measurements with good spatial coverage of a subsurface region, which could complement, or replace, other forms of invasive sampling.

6.3. Geophysical Field-Scale Imaging of Field-Scale Interfaces

[85] The above examples are those where the scale of interfacial phenomena seen at the laboratory scale are also captured in the field-scale measurement. We now review some recent studies where field-scale measurements capture the response of field-scale interfaces. The geophysical detection of field-scale interfaces may, at first glance, not seem new. Seismic reflection and GPR are both methods primarily based on recording energy reflected from interfaces where the bulk (volumetric) properties of the medium change. For example, GPR reflections usually originate from interfaces where water content, being a fundamental control on dielectric constant, changes. Such field-scale interfaces are defined because of a change in the bulk, volumetric geophysical properties. In contrast, we consider here field-scale interfaces where the *interface itself* is responsible for the generation of a detectable geophysical signature. The geophysical investigation of such interfaces is the subject of a growing literature of recent research in near-surface geophysics. We give examples of two field-scale fluid-fluid interfaces; one is an interface separating differences in fluid phases, and the other is an interface separating differences in fluid chemistry.

[86] A field-scale fluid-fluid interface of great interest in subsurface investigations is the water table. For many years geophysicists have strived, with varying success, to identify the water table from the contrast in the bulk geophysical properties (electrical and seismic) between saturated and unsaturated materials as a result of the replacement of the air in the pores with water. For example, under optimal conditions (shallow depths and resistive materials) GPR may be an effective technique to detect the water table because of the response generated by the contrast in dielectric constant [e.g., *Bevan et al.*, 2003]. However, recent research suggests that a more versatile geophysical approach to detecting the water table is based upon recording a unique electrical geophysical signal (a form of self-potential) that can be directly associated with the water table itself.

[87] It is well known that the flow of groundwater produces a streaming current owing to the electrokinetic coupling at the solid-fluid interface that can be recorded, using a set of nonpolarizing electrodes, as a self-potential at the ground surface. Several papers have demonstrated that a measurable self-potential can be directly associated with the shape of the water table surface [*Fournier*, 1989; *Birch*, 1993; *Revil et al.*, 2003]. What drives this hydroelectric coupling is groundwater flow in the gravity field and associated electrokinetic conversion. When observed at the ground surface the water table appears to carry a dipolar momentum with a dipole strength proportional to the piezometric head and the streaming potential coupling coefficient. *Revil et al.* [2003] proposed an inverse scheme to recover the shape of the water table from the dipolar field at this fluid-fluid interface using self-potential measurements made at the ground surface. The water table must be measured in at least one piezometer in order to remove the nonuniqueness of the solution. The inverse problem has been solved recently by *Jardani et al.* [2009] inside a Bayesian framework, and a complete mathematical theory has been developed by *Malama et al.* [2009a, 2009b].

[88] One promising application of this method is the geophysical monitoring of pump tests to recover aquifer parameters that control the availability and flow of groundwater. The analysis of pump tests requires measurements of the drawdown of the water table as a function of elapsed time since pumping. The traditional form of observation using piezometers is often limited by a low number of observation wells, as well as the fact that the piezometer installations may disturb the in situ hydraulic head distribution. *Rizzo et al.* [2004] demonstrated the application of this technique in a field-scale pumping test project where the water table surface was recovered at numerous electrode locations.

[89] An intriguing field-scale fluid-fluid interface that has been attributed to the generation of large self-potentials is the redox gradient at the water table [*Naudet et al.*, 2004]. In order to explain large (~0.4 V) self-potential signals recorded over the Entressen Landfill (France) [*Naudet et al.*, 2003] that could not be explained by electrodiffusional effects, *Naudet et al.* [2004] proposed a conceptual biogeobattery model, whereby the distribution of redox potential across the landfill is associated with a strong redox gradient between highly reducing conditions below the water table within the plume (due to biodegradation and oxygen depletion) and the oxidized zone above the water table. The driving force of this electrochemical cell is dissolved Fe^{2+} resulting from the oxidation of organic matter by bacteria followed by reduction of Fe(III) oxides. To complete the geobattery, *Naudet et al.* [2004] proposed that biofilms forming at the groundwater table could possibly provide the short circuit and required electron transport. The physics of the model was developed by *Arora et al.* [2007], who showed that the source of the current density is indeed the drop in the redox potential across the water table.

[90] *Naudet et al.* [2003, 2004] utilized this self-potential source signal to map the redox distribution associated with a leachate plume emanating from the Entressen landfill. This redox distribution, arising from a field-scale fluid-fluid interface and detected with geophysical measurements, is

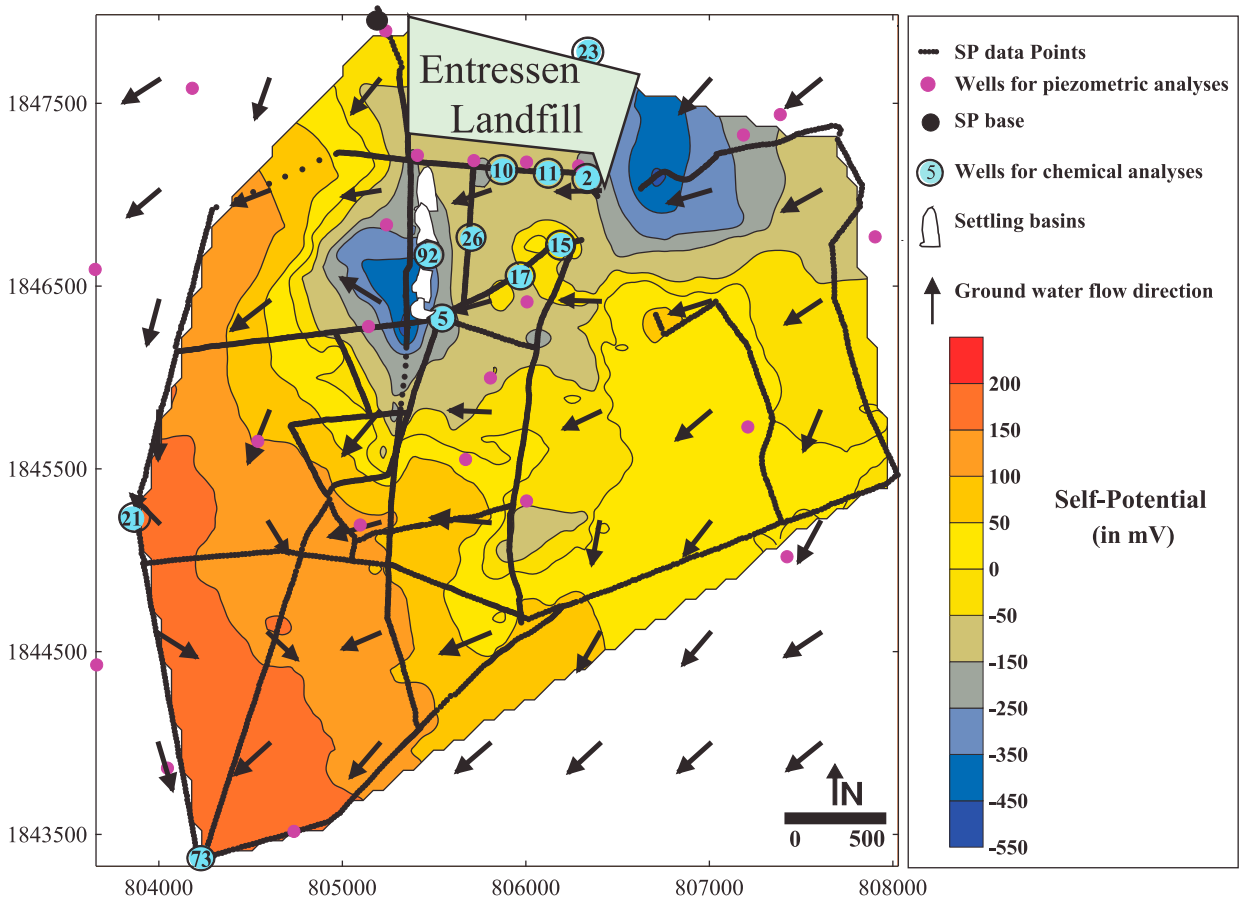

Figure 18. Self-potential signals measured adjacent to a landfill in Entressen in the south of France.

depicted in Figure 18. The in situ measurement of redox potential at landfills is a difficult task (requiring direct emplacement of standard reference electrodes), and the obtained information is usually poorly distributed because of the cost of drilling a large set of sampling wells. Such an application of self-potential measurements is an exciting new use of geophysical data. It also represents a new way of thinking of the geophysical response of the subsurface, with a focus on exploiting the geophysical signatures arising at interfaces, defined by their own unique properties.

6.4. Geophysical Field Measurements: Current Challenges

[91] While Table 1 indicates that we can obtain measurements at a field site of all the geophysical properties discussed in this review, we still face challenges in acquiring, analyzing, and interpreting the data that limit our ability to use geophysical field methods in the new ways suggested in this review for Critical Zone applications.

[92] In terms of the challenges we face in the acquisition of data, the primary limitation is technological; we cannot make the measurement at the scale or resolution needed for Critical Zone applications. An example is the development of a surface-based system for the measurement of NMR. NMR logging has been used for many years for petroleum applications to estimate the properties of petroleum reservoirs such as water-filled porosity, pore size distribution, and permeability [*Seevers*, 1966; *Kenyon et al.*, 1988; *Straley et al.*, 1995]. There is now great interest in the use of surface-based systems, referred to as surface NMR or magnetic resonance sounding, for groundwater applications. Two commercially available systems have been developed that use a loop of wire (~50–100 m in diameter) on the ground surface to generate NMR excitation pulses and to measure relaxation times [*Legchenko et al.*, 2002; *Vouillamoz et al.*, 2002; *Walsh*, 2008]. But the surface-based measurement can only provide a vertical resolution on the order of meters and cannot currently quantify the full range of NMR parameters used in logging NMR. Recent technological advances have included improving the signal-to-noise ratio and reducing the instrument dead time.

[93] Similar technological challenges exist regarding the implementation of the spectral induced polarization (SIP) method in the field. Laboratory measurements have shown the potential to extract hydrological parameters from the frequency dependence (mHz-kHZ) of the electrical properties. However, the acquisition of reliable SIP spectra in the field is extremely challenging as capacitive and electromagnetic coupling often overwhelms the signal at frequencies above a few Hz. Technological advances that utilize fiber optic signal transmission offer the possibility of improving the utility of the SIP method in the field.

[94] An important step in field-scale studies involves inverting the acquired field data to obtain an accurate model of the subsurface in terms of geophysical properties. That is, we need to represent the subsurface in terms of the geophysical properties that can be related (through laboratory and theoretical studies) to Critical Zone properties and processes. The technological advancements over the past decade that have allowed us to acquire larger volumes of data and have greatly expanded computational power have triggered research activity in developing methods to efficiently handle and invert large volumes of data. But there are still limitations in our ability to accurately represent the subsurface 3-D distribution of geophysical properties. For example, we lack reliable methods that allow us to routinely recover the dielectric constant from ground-penetrating radar data. Another example is the inversion of SIP data. Although the inversion of single-frequency IP data is relatively routine, codes for the inversion of SIP data are currently nonexistent. A third example is the inversion of surface-based NMR data, which is a very young field of research, given that the measurement systems were only recently developed.

[95] Inversion of geophysical data provides a nonunique solution; in other words, there are many distributions of subsurface geophysical properties that correspond to any given data set. This means that there will always be some level of uncertainty in the determined magnitude of the geophysical properties and in the estimated magnitude of the related subsurface property. A related issue is the complexity of the subsurface, as probed with field-scale measurements. In the laboratory, the studies that have documented the links between geophysical properties and the properties of an interface have been carefully designed experiments with controlled variation in experimental parameters and conditions. This is rarely, if ever, the case in field experiments where a geophysical measurement responds not to one experimental variable but to many mechanisms contributing to the measurement, at many scales. Given (1) the inherent nonuniqueness in the inversion of geophysical data and (2) the many possible contributions to a single geophysical measurement, it will always be extremely challenging to use a single geophysical measurement to quantify some aspect of the subsurface.

[96] An alternate approach is to use geophysical measurements as a means of monitoring changes. Controlled laboratory studies have provided physical understanding and theoretical methods for interpreting geophysical measurements as a function of measurement parameters (e.g., frequency and field of view), material properties, and time-dependent processes. Time-lapse monitoring of geophysical measurement dramatically simplifies elements of data analysis and interpretation and is an excellent complement to other forms of direct measurement [*Birken and Versteeg*, 2000; *Versteeg and Johnson*, 2008].

[97] An essential step in the use of geophysical field measurements is transforming the representation of the subsurface in terms of geophysical properties to a representation in terms of the properties and processes of interest. In some geophysical field applications, we can acquire the data and obtain accurate models representing the geophysical properties of the subsurface, but we are unsure how to use laboratory-based observations to guide our interpretation of geophysical measurements made at a much larger scale. The laboratory-scale studies provide us with a good understanding of the relationship between, for example, σ'' measured on a core sample and S/V_{pore} measured on a core sample. Is the same relationship valid when σ'' is determined, through inversion of the data, at a scale of a few meters? Methods have been proposed for upscaling the relationship between a geophysical property and the material property of interest [e.g., *Moysey et al.*, 2005]. But this remains an area of research with many unanswered questions and must be addressed if we are to build on laboratory-scale observations and develop new ways of using geophysics for Critical Zone studies.

[98] One of the challenges in the upscaling is adequately accounting for the nature of the heterogeneity at the field scale and determining how the lab-scale properties contribute to the field-scale response. As noted, for example, in the works of *Oliger et al.* [2003] and *Acosta-Colon et al.* [2009], the ability to interpret fracture properties from seismic data requires an understanding not only of the role of fracture specific stiffness but of the effect of probabilistic and spatial distributions of fracture specific stiffness that affect our ability to interpret changes in fracture properties. *Acosta-Colon et al.* [2009] determined that many small-scale measurements of fracture specific stiffness did not predict the large-scale response of the fracture. They observed that a nonuniform spatial distribution of fracture specific stiffness resulted in a scale-dependent seismic response of fracture properties; that is, interpretation of fracture specific stiffness depends on the frequency content of the signal and field of view. Laboratory studies, such as those reported here, provide a fundamental physical understanding of attenuation mechanisms caused by fractures and alterations to fractures, as well as how to unravel competing geometric effects of spatial correlations and probability distributions of fracture specific stiffness. Future areas of research on interpreting fracture properties from field seismic data must include the study of the effect of distributions of fracture specific stiffness within and among sets of fractures and how these distributions affect our ability to interpret changes in fractures caused by time-dependent processes such as changes in stress, fluid phases, microbial interactions, etc.

7. CONCLUSIONS

[99] Over the past decade there has been increasing use of geophysical methods to obtain images of the top ~100 m of Earth. The challenge has always been connecting the geophysical image to the "geological reality." That is, how are the geophysical properties that we measure related to the subsurface properties and processes of interest? And, therefore, how can we best use geophysical measurements to acquire the information that we need about subsurface properties and processes?

[100] As reviewed in this paper, laboratory studies have found that geophysical measurements are very sensitive to the presence and properties of pore-scale solid-fluid, fluid-fluid, and solid-solid interfaces in granular and fractured materials. However, more basic research is needed to improve our understanding of the geophysical signatures arising at interfaces. For example, the response of electrical properties to spatial variability in fluid-fluid interfaces during wetting and drying cycles remains uncertain. The effects of complex spatial distributions of solid-fluid interfaces or spatially varying solid-solid interfaces on seismic wave propagation are also not well understood or accounted for in most geophysical models/theories. Much additional work is also clearly needed to understand how geochemical, biogeochemical, and microbiological processes alter all geophysical signatures of all three interfaces described here. Integration of geophysical measurements (e.g., simultaneous measurements of seismic, electrical, and NMR signals) will likely accelerate such understanding of the geophysical signatures of interfaces.

[101] While we lack a complete understanding of the geophysical signatures of interfaces, the laboratory studies reviewed here clearly suggest that geophysical measurements should be used in new ways to obtain the information required to better understand in situ properties and processes. Field-scale experiments are now required to determine whether the geophysical responses seen in the laboratory can be seen in the field and used for informed interpretation. While such experiments would be challenging, time consuming, and expensive, they are essential to advancing the use of geophysical methods for characterizing the subsurface.

[102] We have included two examples of field-scale studies in which the geophysical target was an interface and the geophysical response was from the interface itself. As seen at the pore scale, a field-scale interface can have unique properties and can affect geophysical data in ways that cannot be accounted for by considering only the responses of the components, or regions, on either side of the interface. A focus on imaging interfaces, which are commonly the target of interest in monitoring subsurface processes, represents a new way of thinking about the acquisition of geophysical data.

[103] Geophysical measurements are sensitive, across a range of scales, to the physical, chemical, biological, and geological changes in a system that affect solid-fluid, fluid-fluid, and solid-solid interfaces. This sensitivity, and our ability to noninvasively obtain high-resolution geophysical images of the top ~100 m of Earth, means that geophysical methods can potentially contribute in many ways to advancing our understanding of the region of Earth referred to as the Critical Zone.

NOTATION

a empirically determined constant in power law describing the dependence of the dielectric constant on frequency.

A measured amplitude of compressional wave.

$A_{\max}$ maximum measured amplitude of compressional wave.

B bulk modulus.

B_0 static magnetic field.

c empirically determined constant in relationship between NMR-derived parameters and permeability.

C coupling coefficient between electrical and pore fluid potentials.

D surface diffusion coefficient.

G interfacial free energy.

IA interfacial area (surface area) of an interface, where subscripts *s/f* and *f/f* refer to a solid-fluid and fluid-fluid interface, respectively.

IAV interfacial area per volume.

k permeability.

K hydraulic conductivity.

l sample length.

m cementation exponent.

M nuclear magnetization.

p pore fluid potential.

P_c capillary pressure.

P wave compressional wave.

Q seismic quality factor.

$\bar{Q}_v$ excess charge of the diffuse layer per pore unit volume.

r hydraulic radius.

R grain radius.

S surface area, i.e., total area of the interface between the void space and the solid phase.

S_f level of fluid saturation, i.e., volume fraction of the pore space filled with fluid.

S_{sv} specific surface (area) defined as the surface area per unit volume of the solid phase.

S_w level of water saturation, i.e., volume fraction of the pore space filled with water.

$S_{w\ \mathrm{crit}}$ level of water saturation below which the dielectric constant shows a significant increase.

S wave shear wave.

S/V_{pore} surface-area-to-volume ratio of the pore space.

T_2 NMR relaxation time constant.

T_{2b} NMR relaxation time constant of bulk liquid.

$T_{2\mathrm{ML}}$ mean log of the T_2 values.

T_{2s} NMR surface relaxation time constant.

T_D NMR time constant associated with diffusion of the hydrogen nuclei in an inhomogeneous magnetic field.

u spectral amplitude for a sample.

u_o spectral amplitude for a standard.

V_p compressional wave (P wave) velocity.

V_{pore} volume of the pore space.

V_s shear wave (S wave) velocity.

V_{phase} phase velocity.

α empirically determined power law exponent describing the dependence of the dielectric constant on frequency.

α_s seismic attenuation coefficient.

γ surface tension of an interface, where subscripts *s/f* and *f/f* refer to a solid-fluid and fluid-fluid interface, respectively.
δ density.
ε_0 permittivity of free space.
κ' dielectric constant.
κ'_{GHz} dielectric constant at frequencies close to 10 GHz; defined as κ' as the frequency of the applied electric field approaches the relaxation frequency (~10 GHz) of bulk water.
κ'_s dielectric constant of the dry solid.
κ'_w dielectric constant of the pore water.
μ shear modulus.
ρ_2 surface relaxivity.
σ total measured complex electrical conductivity.
σ' real part of the total measured complex electrical conductivity.
σ'' imaginary part of the total measured complex electrical conductivity.
σ_{DC} DC conductivity, here defined as the value of σ' as $\omega \rightarrow 0$.
$\sigma_{\mathrm{DC\ water}}$ DC conductivity of the pore water.
τ diffusive relaxation time constant.
ϕ porosity.
φ electrical potential.
ω frequency.

[104] **ACKNOWLEDGMENTS.** This manuscript resulted from the workshop "Geophysical Images of the Near-Surface: What are we really measuring?," which was financially supported by the office of Basic Energy Science of the Department of Energy. We are grateful to Nick Woodward for his encouragement and support throughout the workshop and for his encouragement, support, and patience during the preparation of the manuscript. We also wish to thank Michael Knoll for his contributions to the workshop. We are very grateful to the Editors, Michael Manga and Mark Moldwin, and the reviewers, whose comments led to significant improvements in the manuscript.

[105] The Editor responsible for this paper was Mark Moldwin. He thanks two anonymous reviewers.

REFERENCES

Abdel Aal, G. Z., E. Atekwana, L. Slater, and E. Atekwana (2004), Effects of microbial processes on electrolytic and interfacial electrical properties of unconsolidated sediments, *Geophys. Res. Lett.*, *31*, L12505, doi:10.1029/2004GL020030.

Acosta-Colon, A., L. D. Pyrak-Nolte, and D. D. Nolte (2009), Laboratory-scale study of field of view and the seismic interpretation of fracture specific stiffness, *Geophys. Prospect.*, *57*(2), 209–224, doi:10.1111/j.1365-2478.2008.00771.x.

Archie, G. E. (1942), The electrical resistivity log as an aid in determining some reservoir characterisitics, *Trans. Am. Inst. Min. Metall. Pet. Eng.*, *146*, 54–62.

Arora, T., A. Revil, N. Linde, and J. Castermant (2007), Non-intrusive determination of the redox potential of contaminant plumes using the self-potential method, *J. Contam. Hydrol.*, *92*(3–4), 274–292, doi:10.1016/j.jconhyd.2007.01.018.

Atekwana, E. A., and L. D. Slater (2009), Biogeophysics: A new frontier in Earth science research, *Rev. Geophys.*, *47*, RG4004, doi:10.1029/2009RG000285.

Bennett, P. C., F. K. Hiebert, and W. J. Choi (1996), Microbial colonization and weathering of silicates in a petroleum-contaminated groundwater, *Chem. Geol.*, *132*, 45–53, 2155, doi:10.1016/S0009-2541(96)00040-X.

Bevan, M. J., A. L. Endres, D. L. Rudolph, and G. Parkin (2003), The non-invasive characterization of pumping-induced dewatering using ground penetrating radar, *J. Hydrol.*, *281*(1–2), 55–69, doi:10.1016/S0022-1694(03)00200-2.

Birch, F. S. (1993), Testing Fournier's method for finding water table from self-potential, *Ground Water*, *31*, 50–56, doi:10.1111/j.1745-6584.1993.tb00827.x.

Birken, R., and R. Versteeg (2000), Use of four-dimensional ground penetrating radar and advanced visualization methods to determine subsurface fluid migration, *J. Appl. Geophys.*, *43*, 215–226, doi:10.1016/S0926-9851(99)00060-9.

Bockris, J. O., E. Gileady, and K. Muller (1966), Dielectric relaxation in the electric double layer, *J. Chem. Phys.*, *44*, 1445–1456, doi:10.1063/1.1726876.

Bolève, A., A. Crespy, A. Revil, F. Janod, and J. L. Mattiuzzo (2007), Streaming potentials of granular media: Influence of the Dukhin and Reynolds numbers, *J. Geophys. Res.*, *112*, B08204, doi:10.1029/2006JB004673.

Börner, F. D., and J. H. Schön (1991), A relation between the quadrature component of electrical conductivity and the specific surface area of sedimentary rocks, *Log Anal.*, *32*, 612–613.

Börner, F. D., J. R. Schopper, and A. Weller (1996), Evaluation of transport and storage properties in the soil and groundwater zone from induced polarization measurements, *Geophys. Prospect.*, *44*, 583–601, doi:10.1111/j.1365-2478.1996.tb00167.x.

Borrok, D., J. B. Fein, and C. F. Kulpa (2004), Proton and Cd adsorption onto natural bacterial consortia: Testing universal adsorption behavior, *Geochim. Cosmochim. Acta*, *68*(15), 3231–3238, doi:10.1016/j.gca.2004.02.003.

Bourbie, T., O. Coussy, and B. Zinszner (1987), Acoustics of Porous Media, Ed. Technip, Paris.

Brown, S. R., and C. H. Scholz (1985), Closure of random surfaces in contact, *J. Geophys. Res.*, *90*, 5531–5545, doi:10.1029/JB090iB07p05531.

Brown, S. R., and C. H. Scholz (1986), Closure of rock joints, *J. Geophys. Res.*, *91*, 4939–4948, doi:10.1029/JB091iB05p04939.

Brownstein, K. R., and C. E. Tarr (1979), Importance of classical diffusion in NMR studies of water in biological cells, *Phys. Rev. A*, *19*(6), 2446–2453, doi:10.1103/PhysRevA.19.2446.

Bryar, T. R., and R. J. Knight (2003), Laboratory studies of the effect of sorbed oil on proton nuclear magnetic resonance, *Geophysics*, *68*, 942–948, doi:10.1190/1.1581046.

Bryar, T. R., C. J. Daughney, and R. J. Knight (2000), Paramagnetic effects of iron(III) species on nuclear magnetic relaxation of fluid protons in porous media, *J. Magn. Reson.*, *142*, 74–85, doi:10.1006/jmre.1999.1917.

Carman, P. C. (1956), Flow of Gases Through Porous Media, 182 pp., Academic, New York.

Chapman, M., S. V. Zatsepin, and S. Crampin (2002), Derivation of a microstructural poroelastic model, *Geophys. J. Int.*, *151*(2), 427–451, doi:10.1046/j.1365-246X.2002.01769.x.

Chen, D. Q., L. J. Pyrak-Nolte, J. Griffin, and N. J. Giordano (2007), Measurement of interfacial area per volume for drainage and imbibition, *Water Resour. Res.*, *43*, W12504, doi:10.1029/2007WR006021.

Chen, W.-Y., C. W. Lovell, G. M. Haley, and L. J. Pyrak-Nolte (1993), Variation of shear wave amplitude during frictional sliding, *Int. J. Mech. Min. Sci. Geomech. Abstr.*, *30*(7), 779–784, doi:10.1016/0148-9062(93)90022-6.

Cheng, J. T., L. Pyrak-Nolte, D. D. Nolte, and N. J. Giordano (2004), Linking pressure and saturation through interfacial areas in porous media, *Geophys. Res. Lett.*, *31*, L08502, doi:10.1029/2003GL019282.

Claessens, J., T. Behrends, and P. Van Cappellen (2004), What do acid-base titrations of live bacteria tell us? A preliminary assessment, *Aquat. Sci.*, *66*, 19–26, doi:10.1007/s00027-003-0687-0.

Clark, V. A., B. R. Tittmann, and T. W. Spencer (1980), Effect of volatiles on attenuation (Q^{-1}) and velocity in sedimentary rocks, *J. Geophys. Res.*, *85*(B10), 5190–5198, doi:10.1029/JB085iB10p05190.

Cole, K. S., and R. H. Cole (1941), Dispersion and absorption in dielectrics, *J. Chem. Phys.*, *9*, 341–351, doi:10.1063/1.1750906.

Cox, J. S., D. S. Smith, L. A. Warren, and F. G. Ferris (1999), Characterizing heterogeneous bacterial surface functional groups using discrete affinity spectra for proton binding, *Environ. Sci. Technol.*, *33*(24), 4514–4521, doi:10.1021/es990627l.

Daughney, C. J., and J. B. Fein (1998), The effect of ionic strength on the adsorption of H^+, Cd^{2+}, Pb^{2+}, and Cu^{2+} by *Bacillus subtilis* and *Bacillus licheniformis*: A surface complexation model, *J. Colloid Interface Sci.*, *198*, 53–77, doi:10.1006/jcis.1997.5266.

Davis, C. A., E. Atekwana, E. Atekwana, L. D. Slater, S. Rossbach, and M. R. Mormile (2006), Microbial growth and biofilm formation in geologic media is detected with complex conductivity measurements, *Geophys. Res. Lett.*, *33*, L18403, doi:10.1029/2006GL027312.

DeJong, J. T., M. B. Fritzges, and K. Nusslein (2006), Microbially induced cementation to control sand response to undrained shear, *J. Geotech. Geoenviron. Eng.*, *132*, 1381–1392, doi:10.1061/(ASCE)1090-0241(2006)132:11(1381).

DeJong, J. T., B. M. Mortensen, B. C. Martinez, and D. C. Nelson (2010), Bio-mediated soil improvement, *Ecol. Eng.*, *36*, 197–210.

de Lima, O. A. L., and M. M. Sharma (1992), A generalized Maxwell-Wagner theory for membrane polarization in shaly sands, *Geophysics*, *57*, 431–440, doi:10.1190/1.1443257.

Detwiler, R. L. (2008), Experimental observations of deformation caused by mineral dissolution in variable aperture fractures, *J. Geophys. Res.*, *113*(B8), B08202, doi:10.1029/2008JB005697.

Dukhin, S. S., and V. N. Shilov (1974), *Dielectric Phenomena and the Double Layer in Disperse Systems and Polyelectrolytes*, 192 pp., John Wiley, New York.

Dvorkin, J., G. Mavko, and A. Nur (1991), The effect of cementation on the elastic properties of granular material, *Mech. Mater.*, *12*, 207–217, doi:10.1016/0167-6636(91)90018-U.

Dvorkin, J., A. Nur, and H. Yin (1994), Effective properties cemented granular material, *Mech. Mater.*, *18*, 351–366, doi:10.1016/0167-6636(94)90044-2.

Dvorkin, J., G. Mavko, and A. Nur (1995), Squirt flow in fully saturated rocks, *Geophysics*, *60*(1), 97–107, doi:10.1190/1.1443767.

Endres, A. L. (1998), Estimating the effects of pore geometry and pore fluid species on elastic wave velocity dispersion in rocks using microstructural models, *Explor. Geophys.*, *29*(4), 361–367, doi:10.1071/EG998361.

Endres, A. L., and R. J. Knight (1993), A model for incorporating surface phenomena in the dielectric properties of a heterogeneous medium, *J. Colloid Interface Sci.*, *157*(2), 418–425, doi:10.1006/jcis.1993.1204.

Foley, I., S. A. Farooqui, and R. L. Kleinberg (1996), Effect of paramagnetic ions on NMR relaxation of fluids at solid surfaces, *J. Magn. Reson. A*, *123*, 95–104, doi:10.1006/jmra.1996.0218.

Fournier, C. (1989), Spontaneous potentials and resistivity surveys applied to hydrogeology in a volcanic area: Case history of the Chaîne des Puys (Puy-de-Dôme, France), *Geophys. Prospect.*, *37*, 647–668, doi:10.1111/j.1365-2478.1989.tb02228.x.

Geller, J. T., and L. R. Myer (1995), Ultrasonic imaging of organic liquid contaminants in unconsolidated porous media, *J. Contam. Hydrol.*, *19*(2), 85–104, doi:10.1016/0169-7722(95)00014-M.

Geller, J. T., M. B. Kowalsky, P. K. Seifert, and K. T. Nihei (2000), Acoustic detection of immiscible liquids in sand, *Geophys. Res. Lett.*, *27*(3), 417–420, doi:10.1029/1999GL010483.

Gilbert, Z., and L. J. Pyrak-Nolte (2004), Seismic monitoring of fracture alteration by mineral deposition, paper presented at Gulf Rocks 2004, 6th North American Rock Mechanics Symposium, Am. Rock Mech. Assoc., Houston, Tex.

Green, D. H., and R. Esquivel-Sirvent (1999), Acoustic behavior at the fluid/solid transition of kaolinite suspensions, *Geophysics*, *64*(1), 88–92, doi:10.1190/1.1444534.

Guéguen, Y., and V. Palciauskas (1994), *Introduction to the Physics of Rocks*, Princeton Univ. Press, Princeton, N. J.

Hiebert, F. K., and P. C. Bennett (1992), Microbial control of silicate weathering in organic-rich ground water, *Science*, *258*, 278–281, doi:10.1126/science.258.5080.278.

Hildyard, M. W., and R. P. Young (2002), Modelling seismic waves around underground openings in fractured rock, *Pure Appl. Geophys.*, *159*(1–3), 247–276, doi:10.1007/PL00001253.

Hochella, M. F., and A. F. White (1990), Mineral-water interface geochemistry: An overview, in *Mineral-Water Interface Geochemistry*, *Rev. in Mineral.*, vol. 23, edited by M. F. Hochella and A. F. White, pp. 1–16, Mineral. Soc. of Am., Washington, D. C.

Hopkins, D. L. (1990), The effect of surface roughness on joint stiffness, aperture, and acoustic wave propagation, Ph.D. thesis, Univ. of Calif., Berkeley.

Hopkins, D. L., N. G. W. Cook, and L. R. Myer (1987), Fracture stiffness and aperture as a function of applied stress and contact geometry, in *Rock Mechanics: Proceedings of the 28th US Symposium, Tucson, Arizona*, edited by I. W. Farmer et al., pp. 673–680, A. A. Balkema, Rotterdam, Netherlands.

Hördt, A., R. Blaschek, A. Kemna, and N. Zisser (2007), Hydraulic conductivity estimation from induced polarization data at the field scale—The Krauthausen case history, *J. Appl. Geophys.*, *62*, 33–46, doi:10.1016/j.jappgeo.2006.08.001.

Hwang, Y. K., A. L. Endres, S. D. Piggott, and B. L. Parker (2008), Long-term ground penetrating radar monitoring of a small volume DNAPL release in a natural groundwater flow field, *J. Contam. Hydrol.*, *97*(1–2), 1–12, doi:10.1016/j.jconhyd.2007.11.004.

Jain, V., S. Bryant, and M. Sharma (2003), Influence of wettability and saturation on liquid-liquid interfacial area in porous media, *Environ. Sci. Technol.*, *37*(3), 584–591, doi:10.1021/es020550s.

Jardani, A., and A. Revil (2009), Stochastic joint inversion of temperature and self-potential data, *Geophys. J. Int.*, *179*(1), 640–654, doi:10.1111/j.1365-246X.2009.04295.x.

Jardani, A., A. Revil, W. Barrash, A. Crespy, E. Rizzo, S. Straface, M. Cardiff, B. Malama, C. Miller, and T. Johnson (2009), Reconstruction of the water table from self potential data: A Bayesian approach, *Ground Water*, *47*(2), 213–227, doi:10.1111/j.1745-6584.2008.00513.x.

Johnston, D. H., M. N. Toksoz, and A. Timur (1979), Attenuation of seismic waves in dry and saturated rocks: II. Mechanisms, *Geophysics*, *44*(4), 691–711, doi:10.1190/1.1440970.

Jonscher, A. K. (1975), The interpretation of non-ideal dielectric admittance and impedance diagrams, *Phys. Status Solidi A*, *32*, 665–676, doi:10.1002/pssa.2210320241.

Keating, K., and R. Knight (2007), A laboratory study to determine the effect of iron-oxides on proton NMR measurements, *Geophysics*, *72*(1), E27–E32, doi:10.1190/1.2399445.

Keating, K., R. Knight, and K. Tufano (2008), Nuclear magnetic resonance relaxation measurements as a means of monitoring iron mineralization processes, *Geophys. Res. Lett.*, *35*, L19405, doi:10.1029/2008GL035225.

Kemna, A., A. Binley, and L. Slater (2004), Crosshole IP imaging for engineering and environmental applications, *Geophysics*, *69*, 97–107, doi:10.1190/1.1649379.

Kendall, K., and D. Tabor (1971), An ultrasonic study of the area of contact between stationary and sliding surfaces, *Proc. R. Soc. London, Ser. A*, *323*, 321–340, doi:10.1098/rspa.1971.0108.

Kenyon, W. E., P. I. Day, C. Straley, and J. F. Willemsen (1988), A three-part study of NMR longitudinal relaxation properties of water-saturated sandstones, *SPE Form. Eval.*, *3*, 622–636.

Kitsunezaki, C. (1983), Behavior of plane waves across a plane crack, *J. Min. Coll. Akita Univ., Ser. A*, *3*(6), 173–187.

Kleinberg, R. L., and M. A. Horsfield (1990), Transverse relaxation processes in porous sedimentary rock, *J. Magn. Reson.*, *88*, 9–19.

Knight, R. (1991), Hysteresis in the electrical resistivity of partially saturated sandstones, *Geophysics*, *56*, 2139–2147, doi:10.1190/1.1443028.

Knight, R., and A. Abad (1995), Rock/water interaction in dielectric properties: Experiments with hydrophobic sandstones, *Geophysics*, *60*, 431–436, doi:10.1190/1.1443780.

Knight, R. J., and A. Endres (1990), A new concept in modeling the dielectric response of sandstones: Defining a wetted rock and bulk water system, *Geophysics*, *55*, 586–594, doi:10.1190/1.1442870.

Knight, R., and A. L. Endres (2005), An introduction to rock physics for near-surface applications, in *Near-Surface Geophysics*, vol. 1, *Concepts and Fundamentals*, edited by D. Butler, pp. 31–70, Soc. of Explor. Geophys., Tulsa, Okla.

Knight, R. J., and R. Nolen-Hoeksema (1990), A laboratory study of the effect of pore scale fluid distribution on elastic wave velocities, *Geophys. Res. Lett.*, *17*, 1529–1532, doi:10.1029/GL017i010p01529.

Knight, R., and A. Nur (1987a), The dielectric constant of sandstones, 60 kHz to 4 MHz, *Geophysics*, *52*(5), 644–654, doi:10.1190/1.1442332.

Knight, R., and A. Nur (1987b), Geometrical effects in the dielectric response of partially saturated sandstones, *Log Anal.*, *28*, 513–519.

Knight, R. J., A. Chapman, and M. Knoll (1990), Numerical modelling of microscopic fluid distribution in porous media, *J. Appl. Phys.*, *68*, 994–1001, doi:10.1063/1.346666.

Knoll, M. D., R. Knight, and E. Brown (1995), Can accurate estimates of permeability be obtained form measurements of dielectric properties?, paper presented at Symposium of the Applications of Geophysics to Environmental and Engineering Problems, Environ. and Eng. Geophys. Soc., Orlando, Fla.

Kozeny, J. (1927), Uber kapillare leitung des wassers im boden, *Sitzungsber. Akad. Wiss. Wien*, *136*, 271–306.

Landon, M. (2004), Field quantification of sample disturbance of a marine clay using bender elements, M.S. project, Univ. of Mass., Amherst.

Legchenko, A., J. M. Baltassat, A. Beauce, and J. Bernard (2002), Nuclear magnetic resonance as a geophysical tool for hydrogeologists, *J. Appl. Geophys.*, *50*, 21–46, doi:10.1016/S0926-9851(02)00128-3.

Lesmes, D. P., and K. M. Frye (2001), The influence of pore fluid chemistry on the complex conductivity and induced polarization responses of Berea sandstone, *J. Geophys. Res.*, *106*, 4079–4090, doi:10.1029/2000JB900392.

Lesmes, D. P., and F. D. Morgan (2001), Dielectric spectroscopy of sedimentary rocks, *J. Geophys. Res.*, *106*, 13,329–13,346, doi:10.1029/2000JB900402.

Li, C., P. Tercier, and R. Knight (2001), Effect of sorbed oil on the dielectric properties of sand and clay, *Water Resour. Res.*, *37*, 1783–1793, doi:10.1029/2001WR900006.

Li, X., L. Zhong, and L. J. Pyrak-Nolte (2001), The physics of partially saturated porous media: Residual saturation and seismic wave propagation, *Annu. Rev. Earth Planet. Sci.*, *29*, 419–460, doi:10.1146/annurev.earth.29.1.419.

Liu, C. H., S. R. Nagel, D. A. Schecter, S. N. Coppersmith, S. Majumdar, O. Narayan, and T. A. Witten (1995), Force fluctuations in bead packs, *Science*, *269*, 513–515, doi:10.1126/science.269.5223.513.

Malama, B., K. L. Kuhlman, and A. Revil (2009a), Theory of transient streaming potentials associated with axial-symmetric flow in unconfined aquifers, *Geophys. J. Int.*, *179*, 990–1003, doi:10.1111/j.1365-246X.2009.04336.x.

Malama, B., A. Revil, and K. L. Kulhman (2009b), A semi-analytical solution for trensient streaming potentials associated with confined aquifer pumping tests, *Geophys. J. Int.*, *176*, 1007–1016, doi:10.1111/j.1365-246X.2008.04014.x.

Martinez, R. E., D. S. Smith, E. Kulczycki, and F. G. Ferris (2002), Determination of intrinsic bacterial surface acidity constants using a Donnan shell model and a continuous pKa distribution method, *J. Colloid Interface Sci.*, *253*, 130–139, doi:10.1006/jcis.2002.8541.

Mavko, G., T. Mukerji, and J. Dvorkin (1998), *Rock Physics Handbook*, Cambridge Univ. Press, Cambridge, U. K.

McMahon, P. B., F. H. Chapelle, W. F. Falls, and P. M. Bradley (1992), Role of microbial processes in linking sandstone diagenesis with organic-rich clays, *J. Sediment. Petrol.*, *62*(1), 1–10.

McMahon, P. B., D. A. Vroblesky, P. M. Bradley, F. H. Chapelle, and C. D. Gullett (1995), Evidence for enhanced mineral dissolution in organic acid-rich shallow ground water, *Ground Water*, *33*(2), 207–216, doi:10.1111/j.1745-6584.1995.tb00275.x.

Mindlin, R. D. (1958), Waves and vibrations in isotropic, elastic plates, in *Structural Mechanics*, edited by J. W. Goodier and W. J. Hoff, p. 199, Pergamon, Oxford, U. K.

Moerig, R. (1996), Seismic attenuation in artificial glass cracks: Physical and physicochemical effects of fluids, *Geophys. Res. Lett.*, *23*, 2053–2056, doi:10.1029/96GL02147.

Moysey, S., K. Singha, and R. Knight (2005), A framework for inferring field-scale rock physics relationships through numerical simulation, *Geophys. Res. Lett.*, *32*, L08304, doi:10.1029/2004GL022152.

Murty, G. S. (1975), A theoretical model for the attenuation and dispersion of Stoneley waves at the loosely bonded interface of elastic half spaces, *Phys. Earth Planet. Inter.*, *11*, 65–79, doi:10.1016/0031-9201(75)90076-X.

Nakagawa, S., and M. A. Schoenberg (2007), Poroelastic modeling of seismic boundary conditions across a fracture, *J. Acoust. Soc. Am.*, *122*(2), 831–847, doi:10.1121/1.2747206.

Nakagawa, S., K. T. Nihei, and L. R. Myer (2000), Shear induced conversion of seismic waves across single fractures, *Int. J. Rock Mech. Min. Sci.*, *37*(1–2), 203–218, doi:10.1016/S1365-1609(99)00101-X.

National Research Council (2000), *Seeing Into the Earth: Noninvasive Characterization of the Shallow Subsurface for Environmental and Engineering Applications*, 269 pp., Natl. Acad. Press, Washington, D. C.

National Research Council (2001), *Basic Research Opportunities in Earth Science*, Natl. Acad. Press, Washington, D. C.

Naudet, V., A. Revil, J. Y. Bottero, and P. Bégassat (2003), Relationship between self-potential (SP) signals and redox conditions in contaminated groundwater, *Geophys. Res. Lett.*, *30*(21), 2091, doi:10.1029/2003GL018096.

Naudet, V., A. Revil, E. Rizzo, J. Y. Bottero, and P. Bégassat (2004), Groundwater redox conditions and conductivity in a contaminant plume from geoelectrical investigations, *Hydrol. Earth Syst. Sci.*, *8*(1), 8–22, doi:10.5194/hess-8-8-2004.

Nihei, K. T. (1992), Micomechanics of seismic wave propagation in granular rock, Ph.D. thesis, 176 pp., Univ. of Calif., Berkeley.

Oliger, A., D. D. Nolte, and L. J. Pyrak-Nolte (2003), Seismic focusing by a single fracture, *Geophys. Res. Lett.*, *30*(5), 1203, doi:10.1029/2002GL016264.

Paterson, M. S. (1983), The equivalent channel model for permeability and resistivity in fluid-saturated rock—A re-appraisal, *Mech. Mater.*, *2*, 345–352, doi:10.1016/0167-6636(83)90025-X.

Pride, S. R., J. G. Berryman, and J. M. Harris (2004), Seismic attenuation due to wave-induced flow, *J. Geophys. Res.*, *109*, B01201, doi:10.1029/2003JB002639.

Pyrak-Nolte, L. J. (2007), Fracture anisotropy: The role of fracture-stiffness gradients, *Leading Edge*, *26*(9), 1124–1127, doi:10.1190/1.2780781.

Pyrak-Nolte, L. J., and J. P. Morris (2000), Single fractures under normal stress: The relation between fracture specific stiffness and fluid flow, *Int. J. Rock Mech. Min. Sci.*, *37*(1–2), 245–262, doi:10.1016/S1365-1609(99)00104-5.

Pyrak-Nolte, L. J., L. R. Myer, and N. G. W. Cook (1990), Transmission of seismic waves across single natural fractures, *J. Geophys. Res.*, *95*(B6), 8617–8638, doi:10.1029/JB095iB06p08617.

Pyrak-Nolte, L. J., B. L. Mullenbach, and S. Roy (1996), Interface waves along fractures, *J. Appl. Geophys.*, *35*, 79–87, doi:10.1016/0926-9851(96)00009-2.

Revil, A., and N. Linde (2006), Chemico-electromechanical coupling in microporous media, *J. Colloid Interface Sci.*, *302*, 682–694, doi:10.1016/j.jcis.2006.06.051.

Revil, A., V. Naudet, J. Nouzaret, and M. Pessel (2003), Principles of electrography applied to self-potential electrokinetic sources and hydrogeological applications, *Water Resour. Res.*, *39*(5), 1114, doi:10.1029/2001WR000916.

Rizzo, E., B. Suski, A. Revil, S. Straface, and S. Troisi (2004), Self-potential signals associated with pumping tests experiments, *J. Geophys. Res.*, *109*, B10203, doi:10.1029/2004JB003049.

Santamarina, J. C., V. A. Rinaldi, D. Fratta, K. Klein, Y.-H. Wang, G. C. Cho, and G. Cascante (2005), A survey of elastic and electromagnetic properties of near-surface soils, in *Near-Surface Geophysics*, vol. 1, *Concepts and Fundamentals*, edited by D. Butler, pp. 71–87, Soc. of Explor. Geophys., Tulsa, Okla.

Sato, M., and H. M. Mooney (1960), The electrochemical mechanism of sulphide self-potentials, *Geophysics*, *25*, 226–249, doi:10.1190/1.1438689.

Schoenberg, M. (1980), Elastic wave behavior across linear slip interfaces, *J. Acoust. Soc. Am.*, *68*(5), 1516–1521, doi:10.1121/1.385077.

Schoenberg, M. (1983), Reflection of elastic waves from periodically stratified media with interfacial slip, *Geophysics*, *31*, 265–292.

Schwarz, G. (1962), A theory of the low-frequency dielectric dispersion of colloidal particles in electrolyte solutions, *J. Phys. Chem.*, *66*, 2636–2642, doi:10.1021/j100818a067.

Seevers, D. O. (1966), A nuclear magnetic method for determining the permeability of sandstones, paper L presented at 7th Annual Logging Symposium, Soc. of Petrophys. and Well Log Anal., Tulsa, Okla.

Seifert, P. K., J. T. Geller, and L. R. Johnson (1998), Effect of P wave scattering on velocity and attenuation in unconsolidated sand saturated with immiscible liquids, *Geophysics*, *63*, 161–170, doi:10.1190/1.1444309.

Senturia, S. D., and J. D. Robinson (1970), Nuclear spin-lattice relaxation of liquids confined in porous solids, *SPEJ Soc. Pet. Eng. J.*, *10*, 237–244, doi:10.2118/2870-PA.

Sharma, M. M., A. Garrouch, and H. F. Dunlap (1991), Effect of wettability, pore geometry and stress on electrical conduction in fluid saturated rocks, *Log Anal.*, *32*, 511–526.

Silverstein, D. L., and T. Fort (2000), Prediction of air-water interfacial area in wet unsaturated porous media, *Langmuir*, *16*, 829–834, doi:10.1021/la9815751.

Singurindy, O., and B. Berkowitz (2005), The role of fractures on coupled dissolution and precipitation patterns in carbonate rocks, *Adv. Water Resour.*, *28*(5), 507–521, doi:10.1016/j.advwatres.2005.01.002.

Slater, L., and D. Glaser (2003), Controls on induced polarization in sandy unconsolidated sediments and application to aquifer characterization, *Geophysics*, *68*(5), 1547–1558, doi:10.1190/1.1620628.

Slater, L., and D. P. Lesmes (2002), Electrical-hydraulic relationships observed for unconsolidated sediments, *Water Resour. Res.*, *38*(10), 1213, doi:10.1029/2001WR001075.

Slater, L. D., J. Choi, and Y. Wu (2005), Electrical properties of iron-sand columns: Implications for induced polarization investigation and performance monitoring of iron-wall barriers, *Geophysics*, *70*(4), G87–G94, doi:10.1190/1.1990218.

Slater, L., D. Ntarlagiannis, and D. Wishart (2006), On the relationship between induced polarization and surface area in metal-sand and clay-sand mixtures, *Geophysics*, *71*, A1–A5, doi:10.1190/1.2187707.

Straley, C., C. E. Morriss, W. E. Kenyon, and J. J. Howard (1995), NMR in partially saturated rocks: Laboratory insights on free fluid index and comparison with borehole logs, *Log Anal.*, *36*, 40–56.

Straley, C., D. Rossini, H. J. Vinegar, P. Tutunjian, and C. E. Morriss (1997), Core analysis by low field NMR, *Log Anal.*, *38*(2), 84–94.

Suarez-Rivera, R. (1992), The influence of thin clay layers containing liquids on the propagation of shear waves, Ph.D. thesis, Univ. of Calif., Berkeley.

Taherian, M. R., W. E. Kenyon, and K. A. Safinya (1990), Measurement of the dielectric response of water-saturated rocks, *Geophysics*, *55*, 1530–1541, doi:10.1190/1.1442804.

Taylor, R., and R. Knight (2003), An inclusion-based model of elastic wave velocities incorporating patch scale fluid pressure relaxation, *Geophysics*, *68*, 1503–1509, doi:10.1190/1.1620623.

Ulrich, C., and L. D. Slater (2004), Induced polarization measurements on unsaturated, unconsolidated sands, *Geophysics*, *69*, 762–771, doi:10.1190/1.1759462.

van der Wal, A., M. Minor, W. Norde, A. J. B. Zehnder, and J. Lyklema (1997a), Conductivity and dielectric dispersion of gram-positive bacterial cells, *J. Colloid Interface Sci.*, *186*, 71–79, doi:10.1006/jcis.1996.4615.

van der Wal, A., W. Norde, A. J. B. Zehnder, and J. Lyklema (1997b), Determination of the total charge in the cell walls of Gram-positive bacteria, *Colloids Surf. B*, *9*, 81–100, doi:10.1016/S0927-7765(96)01340-0039.

Versteeg, R., and T. Johnson (2008), Using time-lapse electrical geophysics to monitor subsurface processes, *Leading Edge*, *27*(11), 1488–1497, doi:10.1190/1.3011021.

Vouillamoz, J.-M., M. Descloitres, J. Bernard, P. Fourcassier, and L. Romagny (2002), Application of integrated magnetic resonance sounding and resistivity methods for borehole implementation: A case study in Cambodia, *J. Appl. Geophys.*, *50*(1–2), 67–81.

Walsh, D. O. (2008), Multi-channel surface NMR instrumentation and software for 1D/2D groundwater investigations, *J. Appl. Geophys.*, *66*, 140–150, doi:10.1016/j.jappgeo.2008.03.006.

Wang, G., and K. Sassa (2003), Pore-pressure generation and movement of rainfall induced landslides: Effects of grain size and fine-particle cement, *Eng. Geol.*, *69*, 109–125, doi:10.1016/S0013-7952(02)00268-5.

Wang, J. R., and T. J. Schmugge (1980), An empirical model for the complex dielectric permittivity of soils as a function of water content, *IEEE Trans. Geosci. Remote Sens.*, *GE-18*, 288–295, doi:10.1109/TGRS.1980.350304.

Waxman, M. H., and L. J. M. Smits (1968), Electrical conductivities in oil-bearing shaly sands, *SPEJ Soc. Pet. Eng. J.*, *8*, 107–122, doi:10.2118/1863-A.

Wharton, R. P., G. A. Hazen, R. N. Rau, and D. L. Best (1980), Electromagnetic propagation logging: Advances in technique and interpretation, *Pap. 9267*, Soc. of Pet. Eng., Richardson, Tex.

Xian, C., D. D. Nolte, and L. J. Pyrak-Nolte (2002), Seismic detection of gas in a partially saturated fracture, paper presented at North American Rock Mechanics Symposium and 17th Tunneling Association of Canada Conference, Am. Rock Mech. Assoc., Toronto, Ont., Canada, 8–10 July.

E. Atekwana, Boone Pickens School of Geology, Oklahoma State University, 105 Noble Research Center, Stillwater, OK 74078-3031, USA.

A. Endres, Department of Earth and Environmental Sciences, University of Waterloo, Waterloo, ON N2L 3G1, Canada.

J. Geller and S. Nakagawa, Earth Sciences Division, Lawrence Berkeley National Laboratory, MS 90-1116,1 Cyclotron Rd., Berkeley, CA 94720, USA.

R. Knight, Department of Geophysics, Stanford University, 397 Panama Mall, Stanford, CA 94305-2215, USA. (rknight@stanford.edu)

D. Lesmes, Office of Biological and Environmental Research, U.S. Department of Energy, SC-23.4/Germantown Bldg., 1000 Independence Ave. SW, Washington, DC 20585-1290, USA.

L. J. Pyrak-Nolte, Department of Physics, Purdue University, 525 Northwestern Ave., West Lafayette, IN 47907-2036, USA.

S. A. Revil, Department of Geophysics, Colorado School of Mines, GP, Green Center, 1500 Illinois St., Golden, CO 80401, USA.

M. M. Sharma, Department of Petroleum and Geosystems Engineering, University of Texas at Austin, CPE Bldg., Rm. 5.118, Dean Keeton and Speedway, 1 University Stn. C0300, Austin, TX 78712-0228, USA.

L. Slater, Department of Earth and Environmental Sciences, Rutgers, State University of New Jersey, 101 Warren St., Smith 136, Newark, NJ 07102, USA.

C. Straley, NMR Consultant, 2 Circle Dr. E., Ridgefield, CT 06877, USA.